ISTANBUL TECHNICAL UNIVERSITY ★ GRADUATE SCHOOL OF SCIENCE ENGINEERING AND TECHNOLOGY

INTERACTION OF POLY(VINYL ALCOHOL) AND CHITOSAN COATED IRON OXIDE NANOPARTICLES WITH CELL MEMBRANE MODELS

M.Sc. THESIS

Arife KUŞBAZ

Department of Nano Science & Nano Engineering

Nano Science & Nano Engineering Programme

JULY 2018

ISTANBUL TECHNICAL UNIVERSITY ★ GRADUATE SCHOOL OF SCIENCE ENGINEERING AND TECHNOLOGY

INTERACTION OF POLY(VINYL ALCOHOL) AND CHITOSAN COATED IRON OXIDE NANOPARTICLES WITH CELL MEMBRANE MODELS

M.Sc. THESIS

Arife KUŞBAZ
513151003

Department of Nano Science & Nano Engineering

Nano Science & Nano Engineering Programme

Thesis Advisor: Assoc. Prof. Dr. Fatma Neşe KÖK
Thesis Co-Advisor: Assoc. Prof. Dr. Sevim İŞÇİ TURUTOĞLU

JULY 2018

İSTANBUL TEKNİK ÜNİVERSİTESİ ★ FEN BİLİMLERİ ENSTİTÜSÜ

POLİ(VİNİL ALKOL) VE KİTOSAN KAPLI DEMİR OKSİT NANO PARÇACIKLARININ HÜCRE ZARI MODELLERİ İLE ETKİLEŞİMLERİ

YÜKSEK LİSANS TEZİ

Arife KUŞBAZ
513151003

Nano Bilim & Nano Mühendislik Anabilim Dalı

Nano Bilim & Nano Mühendislik Programı

Tez Danışmanı: Doç. Dr. Fatma Neşe KÖK
Eş Danışman: Doç. Dr. Sevim İŞÇİ TURUTOĞLU

TEMMUZ 2018

Arife KUŞBAZ, a M.Sc. student of ITU Graduate School of Science Engineering and Technology student ID 513151003, successfully defended the thesis entitled "INTERACTION OF POLY(VINYL ALCOHOL) AND CHITOSAN COATED IRON OXIDE NANOPARTICLES WITH CELL MEMBRANE MODELS", which she prepared after fulfilling the requirements specified in the associated legislations, before the jury whose signatures are below.

Thesis Advisor :	**Assoc. Prof. Dr. Fatma Neşe KÖK** Istanbul Technical University	.....
Co-advisor :	**Assoc. Prof. Dr. Sevim İŞÇİ TURUTOĞLU** Istanbul Technical University	……..
Jury Members :	**Prof. Dr. Esra ÖZKAN ZAYİM** Istanbul Technical University	.....
	Prof. Dr. Sedef TUNCA GEDİK Gebze Technical University	.....
	Prof. Dr. Melek ÖZKAN Gebze Technical University	.....

Date of Submission : 16 July 2018
Date of Defense : 20 July 2018

To my father,

FOREWORD

I would like to thank my supervisor Assoc. Prof. Dr. Fatma Neşe Kök for her encouragement and support throughout my study. I would like to express my gratitude for her invaluable scientific guidance with her endless patience and smile. I am indebted her for giving me the chance in her research group.

I would like to thank my co-advisor Assoc. Prof. Dr. Sevim İşçi Turutoğlu to teach me about iron oxide nanoparticles and their characterizations.

I am grateful for guidance to Abdulhalim Kılıç who has been helpful and friendly to me, for sharing his knowledge.

I would like to thank Maide Gökçe Bekaroğlu for helps in Rheology Lab.

I would like to thank Reyhan Şengür and Mümin Balaban for their kind friendship and helpfulness.

I would like to specially thank valuable lab friends who are Ayşe Buse Özdabak, Şebnem Seherler and Ceren Kutlu. They always believed me and gave me morale support. I am very lucky to have them.

I would like to thank Feyza Nur Büyüknalçacı, İpek İrem Aykın and Dilara Öztürk for their kind friendship and helpfulness.

I would like to acknowledge Ece Çağdaş, Şeyma Varınca, Elifcan Zengin, İbrahim Özoğuz, Alican Topaloğlu, Doğuş Altunöz, Gönül Seyhan, Öznur Pehlivan, Dilan Demir and Merve Aydın. They make MOBGAM like home.

I owe like to deepest gratitude to my family, my mother Mahi, my brothers Fatih and Mustafa, my sisters Nermin and Emine, my nieces İrem, Zeynep Betül and Fatma Beyza for giving me strength, support and love throughout my life.

Finally, I would like to special thank to my lovely father for teaching to me everything all his life. I feel his hands on my shoulders every time.

July 2018

Arife KUŞBAZ
(Chemist)

TABLE OF CONTENTS

Page

ABBREVIATIONS

MNP : Multifunctional Magnetic Nanoparticle
IOP : Iron Oxide Nanoparticle
DLS : Dynamic Light Scattering
FTIR : Fourier Transform Infrared Spectroscopy
QCM-D : Quartz Crystal Microbalance with Dissipation.
PVA : Poly(vinyl Alcohol)
C : Chitosan
PVA-IOPs : PVA-coated IOPs
C-IOPs : Chitosan-coated IOPs
PBS : Phosphate Buffer Saline
DOTAP : 1,2-dioleoyl-3-trimethylammonium-propane
PC : Phosphatidylcholine
PS : Phosphatidylserine
FDA : The U.S. Food and Drug Administration
WHO : World Health Organization
PVAc : Poly(vinyl Acetate)
DA : Degree of deacetylation

SYMBOLS

f	**:** Frequency
Δf	**:** Frequency change
D	**:** Dissipation
ΔD	**:** Dissipation change
R_{SPM}	**:** Superparamagnetic radius
R_{SD}	**:** Single domain radius
Pa	**:** Pascal
U	**:** Electrophoresis
ζ	**:** Zeta Potential
ε	**:** Permittivity
C	**:** Sensitivity constant

LIST OF TABLES

Page

LIST OF FIGURES

Page

INTERACTION OF POLY(VINYL ALCOHOL) AND CHITOSAN COATED IRON OXIDE NANOPARTICLES WITH CELL MEMBRANE MODELS

SUMMARY

Nanotechnology is being used at different fields from energy to food industry but its application to medical field, such as tissue engineering, bioimaging, drug design, diagnosis, is more recent. According to the World Health Organization (WHO), 8.8 million people were reported dead because of the cancer in 2015. Cancer can be treated with chemotherapy, radiotherapy and surgery but these treatment methods have serious side effects since cancer drugs are not selective so they affect both healthy and cancerous cells. One of the approaches to reduce the toxic side effects and improve patient life quality is the implementation of nanotechnology to the development of new drugs and therapies.

Magnetic nanoparticles are usually made up of nickel, cobalt and iron. Because of their magnetic properties, they can be transferred to desired location with the help of external magnetic field. Generally, magnetite, hematite, maghemite and goethite are known as iron oxides types. Iron oxide nanoparticles (IOPs) are commonly preferred as MRI agent, and targeted drug design. They are, however, toxic and cause problem in physiological environment because of their negative surface charge, easy agglomeration, low stability, and free radical formation. Therefore, they should be modified to reduce their toxicity and coating their surface with polymers is an effective method proposed by different groups.

In this study, iron oxide nanoparticles were coated with two different polymers and the interaction of these particles with cells were studied using artificial cell membrane models. For this purpose, chitosan and poly(vinyl alcohol) (PVA) were selected because of their biodegradable and biocompatible characteristics. Polymers were coated on IOPs surfaces by adsorption method because of its high efficiency and simplicity. In this method, polymer solutions at different concentrations were mixed with IOPs. Optimal polymer concentration was determined according to colloidal stability. Characterizations of the IOPs were done using different techniques. Zeta potential was measured to determine the surface charges, and stability, rheology to observe flow behavior, Dynamic Light Scattering (DLS) to measure particle size, and Fourier Transform Infrared Spectroscopy (FTIR) to investigate binding between IOPs and polymers. After the characterization, interaction between cell and coated and uncoated IOPs were investigated with liposome, a simple biomimetic cell membrane model. Quartz Crystal Microbalance with Dissipation (QCM-D) is used to investigate these interactions in real time and label-free. QCM-D uses piezoelectric effect of quartz crystal. When voltage is applied, quartz crystal oscillates with a defined frequency and this frequency is sensitive to the amount of material attached to the surface. Adsorption/desorption or solid/liquid interaction can be observed according to the frequency shift (Δf). QCM-D also measures viscoelastic properties of adsorbed particles on surface with changes of dissipation (ΔD) at the same time. In this thesis, the interaction of PVA and

chitosan fully coated, partially coated, and uncoated IOPs were investigated with neutral, positive and negatively charged liposome layers. By using QCM-D, interactions of particles with cell were estimated in a shorter time and cheaper than cell culture experiments. Results show that, coating properties, structure and charge of lipids affect the interactions between them and electrostatic interactions are significant parameter.

In the future studies, chemotherapeutic drug loaded particles can be studied both in QCM-D and cell culture to see their effect to the cells.

POLİ(VİNİL ALKOL) VE KİTOSAN KAPLI DEMİR OKSİT NANO PARÇACIKLARININ HÜCRE ZARI MODELLERİ İLE ETKİLEŞİMLERİ

ÖZET

Nanoteknoloji hayatın birçok alanında kullanılmaktadır ama doku mühendisliği, ilaç tasarımı, biyo görüntüleme ve tedavi gibi tıbbi alanlarda kullanımı daha yenidir. Araştırmacılar tedavisi zor olan ya da hiç olmayan hastalıklara çözüm bulabilmek ve var olan tedavileri daha etkin hale getirmek için nanoteknolojiyi bu alanlara uygulamaya başlamışlardır.

Dünya sağlık örgütünün yaptığı bir araştırmaya göre dünya genelinde 2015 yılında 8,8 milyon kişi kanser nedeniyle hayatını kaybetmiştir. Kanser kemoterapi, radyoterapi veya ameliyat ile tedavisi yapılmaya çalışılan bir sağlık problemidir. Bu tedavi yöntemlerinin hastayı iyileştirmesinin yanında birçok yan etkisi de bulunmaktadır. Kemoterapi sırasında hastaya verilen ilaçlar seçici özellikleri olmaması sebebiyle sadece kanserli hücreleri değil, sağlıklı hücreleri de öldürmekte ve tedavi sırasında ya da tedavi sonrasında bağışıklık sistemlerinde ortaya çıkan zayıflıklar ikincil büyük sorunlara yol açmaktadır. Bilim insanları kemoterapi ilaçlarının yan etkilerini azaltabilmek ve tedavi sonrasında hastaların hayat kalitelerini artırmak için nanoteknoloji ile geliştirilmiş ilaçlar ve tedavi yöntemlerini araştırmaya başlamışlardır.

Manyetik nano parçacıklar demir, nikel, kobalt gibi maddelerden oluşan nano boyutlardaki malzemelerdir. Dışarıdan uygulanacak olan manyetik alan ile bu manyetik nano parçacıklar istenilen bölgeye çekilip orada toplanmaları sağlanabilir. Manyetik nano parçacıklar boyutlarının çok küçük olmasından dolayı biyolojik bariyerleri daha kolay aşabilirler ancak toksik özellikleri ve kolay agregasyona uğramaları nedeni ile insan vücudunda modifiye edilmeden kullanılmaları mümkün değildir. Bu etkinin azaltılması için parçacıkların polimerlerle kaplanması en çok kullanılan yöntemlerdendir.

Demir oksit nano parçacıkları su ile dispers edilerek koloidal bir sistem haline getirilirler. Koloidal kararlılığı sağlayabilmek için elektriksel ve sterik stabilizasyon yöntemleri kullanılarak parçacıklar uygun hale getirilmelidir. Elektriksel stabilizasyonu sağlamak için negatif yüklü parçacıklar zıt yüklü polimerle kaplanabilir. Parçacıkların üzerine tutunan polimerler parçacık yüzeylerini tamamen kaplamaları durumunda polimerlerin sahip oldukları elektriksel yükler nedeni ile parçacıklar arası itmelere neden olacaktır. Bu itmeler parçacıkların ortamda asılı kalmasına yani çökmemesine ve parçacıkların birbirlerine yapışmamasına neden olacaktır. Bu tür etkiler elektriksel stabilizasyon olarak isimlendirilir. Sterik stabilizasyon ise koloidal kararlılığı etkileyen bir diğer faktördür. Yüksüz polimer ortamdaki difüzyon kuvvetlerinin etkisi ile parçacık yüzeylerine tutunurlar ve yine aynı sebepten yüzeylerini kapladıkları parçacıklar arası itme kuvvetleri oluştururlar.

İtme kuvvetleri elektriksel stabilizasyon da olduğu gibi kümeleşmeleri ve çökmeleri engellemektedir. Bu yüzden koloidal kararlılık için tez boyunca elektriksel ve sterik etkenler üzerine çalışılıp gerekli testler yapılmıştır.

Bu çalışmada demir oksit nano parçacıkların toksisitesini azaltmak için iki farklı polimer ile kaplama yapıldı. Bunlardan biri bir biyopolimer olan kitosan, diğeri sentetik bir polimer olan poli(vinil alkol) (PVA) dür. Kaplama yapılırken adsorpsiyon yönteminden yararlanılarak hazırlanan demir oksit ve polimer çözeltileri belirli konsantrasyonlar da karıştırılıp kimyasal analiz, parçacık boyutu ve yükü, reolojik davranış gibi karakterizasyon işlemleri yapıldı. Adsorpsiyon yöntemi kolay, ucuz, yüksek verimlilikte gerçekleşen bir yöntem olduğu için tercih edildi.

Parçacıkların yüzeylerinin kaplanması durumları zeta potansiyel ile mobil yükler ölçülerek anlaşılmaya çalışıldı, reoloji verileri ile koloidal yapıda olan bu parçacıkların akış durumları ve agregasyonu hakkında bilgi almak amaçlandı. Parçacık boyutu ölçülerek agregasyona yatkın olan demir oksit nano parçacıkların polimer ile kaplandığında agregasyonu azaltıp azaltmadığı takip edildi. Kullanılan polimerlerin pH değişikliklerinden faydalanılarak, kaplama sürecinin pH değişimlerinden nasıl etkilendiği de araştırıldı. Geleneksel karakterizasyon yöntemleri ile kaplama işleminin başarılı bir şekilde yapıldığının teyit edilmesinden sonra bu parçacıkların hücrelerle etkileşimi hücre zarını taklit eden yapay hücre zarı modeli lipozomlar ile incelendi.

Etkileşimlerin incelenmesinde kullanılan disipasyon ekli kuvars kristal mikroterazi (QCM-D) cihazı piezoelektrik sisteme dayalı, etiketlemeye ihtiyaç olmadan tayin yapan bir yöntem sunmaktadır. Sensor yüzeyine bağlanan nanogram miktarlarda parçacıkları dahi algılayabilen adsorpsiyon/desorpsiyon ya da katı/sıvı etkileşimlerin incelenmesinde kullanılabilen bir cihazdır. İnceleme sırasında adsorpsiyon ya da desorpsiyon değişimleri altın yüzeyinin üzerinde bulunan sabit rezonans frekans değerlerine sahip farklı harmoni değerlerindeki değişimleri ölçüp frekans değişimi (Δf) ve yüzeyde bulunan katmanın viskoelastik ya da rijit bir özellikte olduğunun bilgisini veren disipasyon değişimi (ΔD) değerlerini vermektedir. Bu bilgilerden yola çıkarak parçacıkların nasıl bir yüzeye ne tür bir etki yaptıkları incelenebilir.

In vitro hücre analizleri, yeterli teknik tecrübesi olan kişilerin yapmasını gerektiren ve sonuçları hücre kaynağı, yaşı gibi pek çok faktöre bağlı yöntemlerdir. Ayrıca malzemelerinin pahalı olması, kontaminasyon riski, sonuç alınmasının uzun sürmesi ve etkileşimlerin izlenmesi için etiketlemeye ihtiyaç duyulması araştırmacıları alternatif yöntemler aramaya sürüklemiştir. QCM-D cihazı kullanılarak daha kısa ve ekonomik bir şekilde parçacıkların canlı ile olan etkileşiminin tahmin edilmesi ve hücre deneyleri gibi pahalı ve uzun deneylerin azaltılabilmesi için bir yöntem geliştirilmesi bu sebeple önemlidir.

Bu tez çalışmasında PVA ve kitosan kaplı demir oksit nano parçacıklarının nötr, pozitif ve negatif lipozomlar ile etkileşimleri QCM-D ile incelendi. Yapılan çalışmalar hem kaplama özelliklerinin, hem de lipit membranın yapısının etkileşimi etkilediği ve elektrostatik etkileşimlerin önemli bir parametre olduğunu gösterdi.

Parçacıkların birbirleri üzerinde olan etkileşimleri ise önemli konulardan biridir. Parçacıkların birbirlerini itmesi sonucunda agregasyon önlenmiş böylece koloidal stabilize sağlanmıştır. Stabilizasyonun tersi, agregasyon olması durumunda parçacıkların yüzey yükleri değişir ve boyutları büyür. QCM-D ile yapılan çalışmalar parçacık boyutlarının da en az yükleri kadar etkileşimi değiştirdiğini gösterdi.

Sonuç olarak tez çalışmasında demir oksit nano parçacıklarının polimerler ile kaplanarak toksisitesi ve agregasyonu gibi özellikleri azaltılmaya çalışıldı, farklı pH durumlarındaki sonuçları incelendi ve koloidal karakterizasyonları yapıldı. Hücre deneyleri yapılmadan hücre-nano parçacık etkileşimlerinin incelenmesini sağlamak için QCM-D kullanılarak yapay hücre zarını taklit eden lipozom tabakası üzerinde deneyler yapıldı. Bu sistemin çeşitli boy ve yükte nano parçacıkların farklı özellikte membranlarla etkileşimlerindeki farkların gözlenmesinde kullanılabileceği görüldü.

İleride yapılması düşünülen çalışmalar ise kemoterapi ilaçlarının yüklenmesi ile ilaç varlığındaki davranışlarının QCM-D ile incelenmesi ve *in vitro* hücre deneyleri ile desteklenmesidir.

1. INTRODUCTION

Nanotechnology is being used in different fields from energy to food industry but its application to the medical field, such as tissue engineering, bio imaging, drug design, diagnosis, is recent. Cancer is a dangerous disease and despite the improvements in its treatment, the fatality rate is still high. Chemotherapy is a treatment for cancer, and chemotherapeutic drugs have many disadvantages such as non-specificity, which causes toxicity to healthy cells yielding many side effects. To overcome these disadvantages of chemotherapeutic drugs, many research groups try to find new generation, side specific, and controllable drug delivery systems. Side specific delivery can be provided with different systems and multifunctional magnetic nanoparticles (MNPs) are one of them. Many medically important agents can be attached to MNPs surface and MNPs can be located on the tumor side with applied external magnetic field, which allow the release of the drug only to the tumor surface. Magnetic nanoparticles are made up of iron, nickel, and cobalt. Most commonly used iron oxides are magnetite (Fe_3O_4), maghemite (γ-Fe_20_3), hematite (α-Fe_2O_3), and goethite.

Iron oxide nanoparticles (IOPs) have many properties, which make them useful in biomedical applications such as magnetic properties, easy surface modifications, biocompatibility in low doses, easy fabrication in several sizes and shapes, etc. These properties of IOPs are also used to design the targeted drug delivery systems. In addition, IOPs are used for imaging and magnetic hyperthermia (Sonvico et al, 2005).

IOPs have also some disadvantages. There are various shapes and sizes of IOPs, however, small sizes can accumulate in cell causing toxicity. Moreover, IOPs can produce free radicals; they affect many systems, especially neural system, negatively. IOPs are very important particles but these properties must be modified to reduce the negative effects. One of the most effective methods to reduce toxicity is the surface coating of the nanoparticles (Mahmoudi et al, 2010).

IOPs possess negatively surface charged. This situation causes to cytotoxicity above a certain threshold amount. Uncoated IOPs are low solubility and less stable precipitation in aqueous media. To reduce the toxicity of IOPs can be coated with biopolymers or polymers (Mahmoudi et al, 2011).

1.1 Purpose of Thesis

In this study, the purpose was to have stable and fully covered surfaces of IOPs by controlling the colloidal properties with poly(vinyl alcohol) (PVA) and chitosan and investigate the interaction of constructed IOPs on liposome layer by Quartz Crystal Microbalance with Dissipation (QCM-D) technique by comparing with uncoated IOPs. The interaction between polymers and IOPs can define the flow properties of the system, zeta potential, particle size and chemical interactions. Characterized colloidal stable IOPs (both coated and uncoated) were investigated on negative, neutral and positive charged liposome layer by monitoring changes of frequencies and dissipations with QCM-D.

2. BACKGROUND INFORMATIONS

Specific magnetic, electronic and reduced size properties provide many advantageous of nanoparticles. Size, structure, shape, crystallinity, synthesis methods and chemistry are affected by magnetic nanoparticles. The most popular magnetic materials are nickel, iron and cobalt compounds (Leslie-Pelecky & Rieke, 1996).

2.1 Magnetic Properties

Magnetic dipole moments of unmagnetized material are randomly orientated. When the magnetic field is applied to these materials, the dipole moment can be aligned parallel or antiparallel etc. These various alignments are used to categorize these materials such as diamagnetic, paramagnetic, ferromagnetic and superparamagnetic (Ayyappan et al, 2018).

When magnetic field is applied on the diamagnetic materials, they align opposite to the magnetic field. Paramagnetic materials, on the other hand, are aligned with parallel to the magnetic fields. In ferromagnetism, certain electrically uncharged materials strongly attract others. There are two materials in nature: magnetite or iron oxide (Fe_3O_4) and iron. These materials can be magnetized by an external magnetic field and remain magnetized even after the external field is removed, so called as natural magnets (Jakubovics et al, 1994). Table 2.1 explains the types of particles magnetic behaviors.

Table 2.1: Types of particles magnetic behaviors (Jiles, 1998).

Type	Spin alignment
Diamagnetism	Spins tend to align antiparallel to external magnetic field
Paramagnetism	Spins tend to align parallel to external magnetic field
Ferromagnetism	All spins parallel to one another

2.1.1 Iron oxides (IOs)

The most popular iron oxides are magnetite (Fe_3O_4) and maghemite (γ-Fe_2O_3). Magnetite (International Union of Pure and Applied Chemistry (IUPAC) name: Iron (II, III) oxide) is black or grayish material. It includes divalent and trivalent Fe ions. The chemical formulas are Fe_3O_4 or $FeO.Fe_2O_3$. Magnetite can be oxidized and transformed into maghemite. Maghemite contains only trivalent Fe ions and its IUPAC name is iron (III) oxide. The chemical formula is γ-Fe_2O_3 and has a brownish color (Laurent et al, 2010).

Fe_3O_4 particles shows superparamagnetic properties which is crucial for drug delivery applications. Superparamagnetic materials become magnetized upon exposure to a magnetic field but have no permanent magnetization when the field is turned off. Hence superparamagnetic particles have zero coercivity and no hysteresis.

Size of the nanoparticles is important for determining properties of the systems. Magnetic moments of magnetic nanoparticles affected the size of the particles. Superparamagnetic radius (R_{SPM}) and single domain radius (R_{SD}) is used as a magnetic scale length. R_{SPM} is the maximum radius up to and R_{SD} is the minimum or below (Laurent et al, 2010). Table 2.2 shows the magnetic length of magnetic nanoparticles.

Table 2.2: Characteristic magnetic length scales for iron, maghemite and magnetite (Coey, 2009).

	R_{SD} (nm)	**R_{SPM} (nm)**
Maghemite (γ-Fe_2O_3)	42.5	17.5
Magnetite (Fe_3O_4)	52.7	12.2
Iron	8.3	8.0

2.1.1.1 Therapy with iron oxide nanoparticles (IOPs)

IOPs are generally used in targeted drug delivery as an alternative or together with conventional targeted delivery systems such as liposomes, dendrimers, micelles etc. IOPs can be used to carry bioactive materials both *in vitro* and *in vivo* (Krishnan, 2010).

In addition, IOPs are used in thermotherapy for a solid tumor. Therapy starts with an applied external magnetic field to locate particles to tumor surface and then the temperature is increased up to 41- 46°C. The high temperature causes apoptosis or cellular hyperthermia. Figure 2.1 (a) shows that magnetic nanoparticles including bioactive materials can be injected to the patients and applied external magnetic field can be used to accumulate particles on the tumor region. In Figure 2.1 (b), after the accumulation, temperature is increased, bioactive materials are released to tumor surface and tumor cells were eradicated by high local temperature (Thanh, 2011).

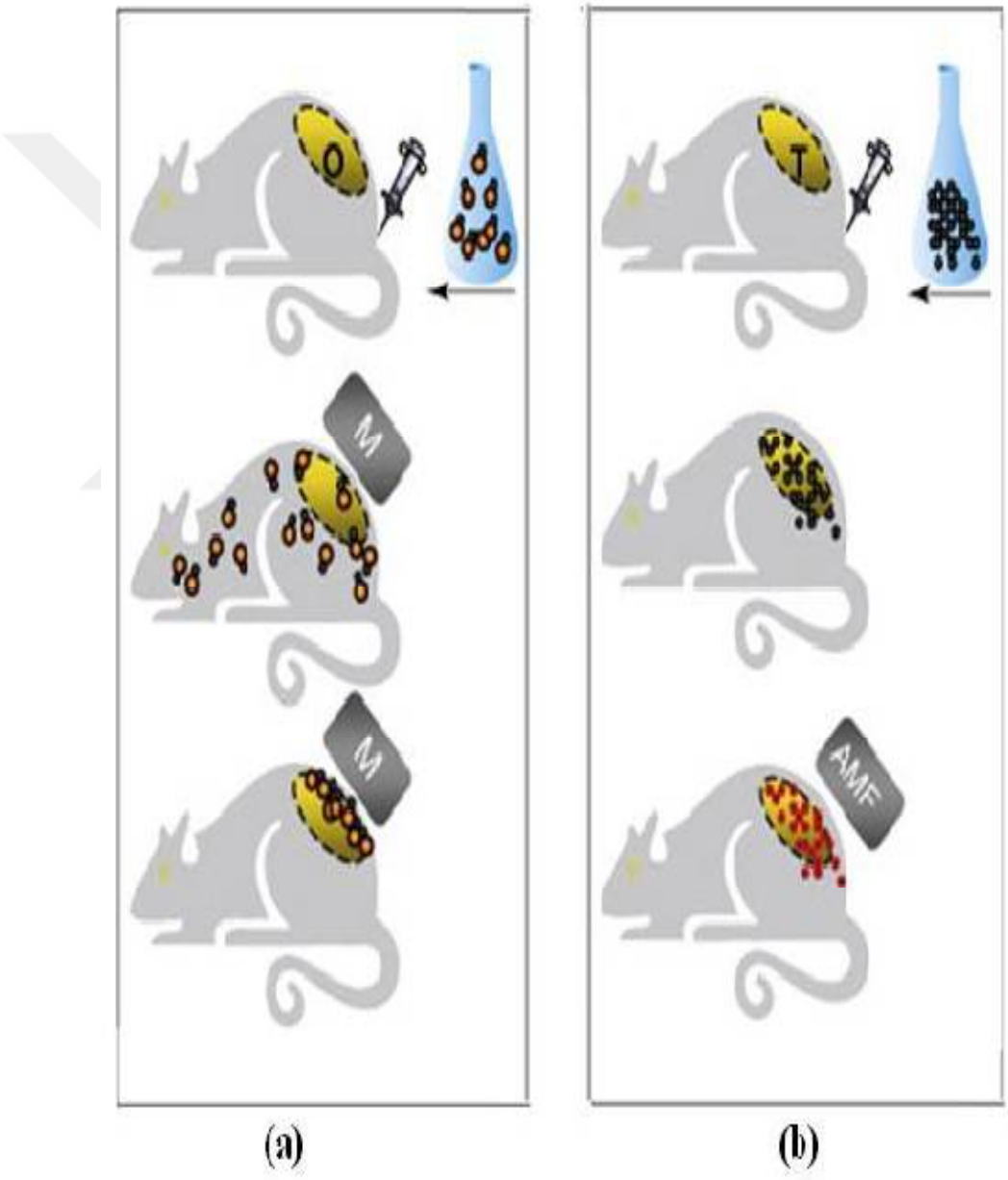

Figure 2.1: Thermotherapy with magnetic nanoparticles (a) first stages of therapy and (b) last stages of therapy (Lee et al, 2011).

2.2 Colloids

The term "colloid" was coined by the Scottish chemist Thomas Graham in 1861 to define the suspensions of liquid or solid phases in another liquid. At present, the colloid is used for dispersed insoluble particles throughout another liquid substance (Jordan et al, 1999).

Sizes of colloidal particles are in range of 10^{-3} to 1 μm (Brandenburg & Lagaly, 1988). Although the colloidal systems look homogenous, they are actually heterogeneous.

Colloidal systems include dispersed phase and a dispersing medium. Colloidal systems are classified according to differences of dispersed phases and dispersing mediums. Classifications of colloids are shown in Table 2.3 (Everett, 1988).

- Dispersing medium (external phase) which is found the major group in the colloid.
- Dispersed phase (internal phase) which is found the minor group in the colloid.

Table 2.3: Types of colloidal systems (Everett, 1988).

Dispersing Medium	Dispersed phase	Name
Solid	Solid	Solid sol
Solid	Liquid	Gel
Solid	Gas	Solid foam
Liquid	Solid	Sol
Liquid	Liquid	Emulsion
Liquid	Gas	Foam
Gas	Solid	Solid, aerosol
Gas	Liquid	Aerosol

A suspension is a special type of dispersion in which solid is dispersed in a liquid phase. Cement and paste are examples can be for colloidal suspensions (Schramm, 1996). The characteristic properties of colloidal suspensions can be understood by

investigating the interactions between particles. Water is a typical suspending liquid. When colloidal particles are suspended in water, two types of interaction, repulsion or attraction, may occur. In the first case, colloidal particles repel each other and prevent the formation of larger and faster agglomerates, therefore, they form stable suspensions. They are shown in Figure 2.2 (Zeta-Meter, Inc., Staunton, VA).

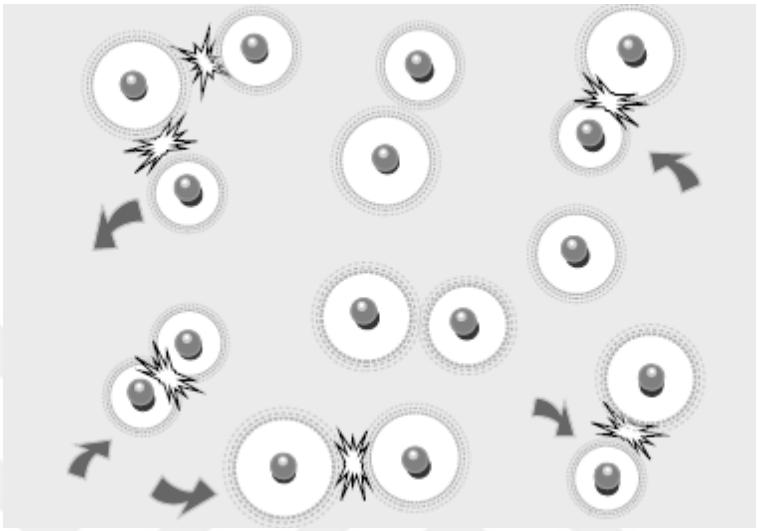

Figure 2.2: Charged particles repelling each other to form stable suspension.

On the other hand, colloidal particles attract each other and stick together as follows: first, dimers and trimers will form. Then, the particles interacts more and they form larger flocs (or cluster, aggregates). Consequently, the flocs continue to grow and sedimentation occurs. They are shown in Figure 2.3 (Zeta-Meter, Inc., Staunton, VA). Under these conditions, the suspension is unstable (McBride et al, 1997).

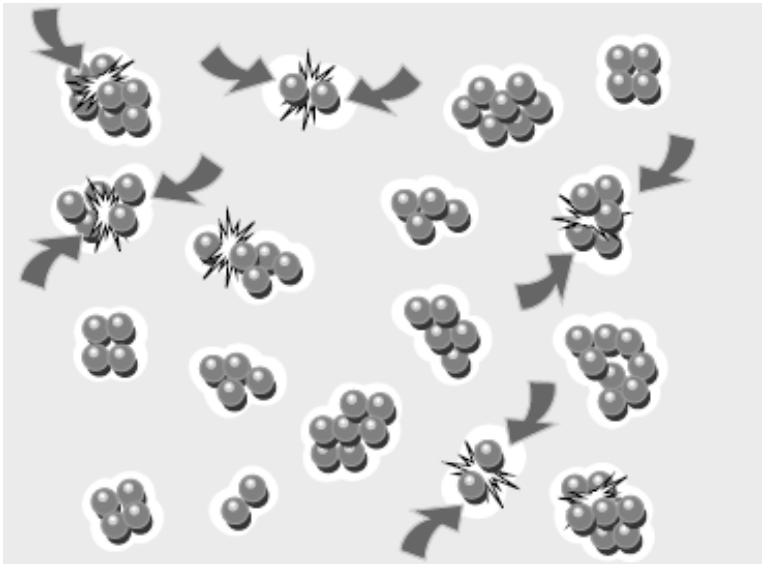

Figure 2.3: Uncharged particles are free to collide and aggregate.

Colloidal behavior in stable (a) and unstable suspensions (b-d) are depicted in Figure 2.4.

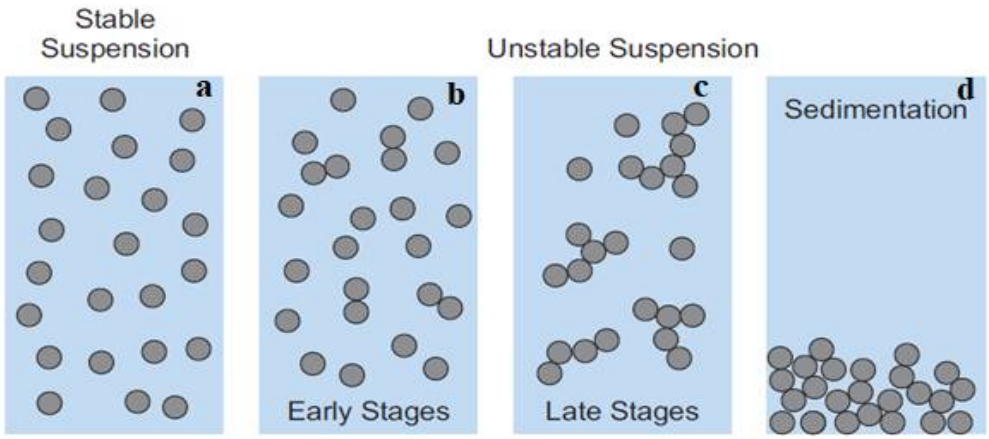

Figure 2.4: Stable and unstable suspensions behaviors (Trefalt & Borkovic, 2014).

Size, charge, shape and interface properties are the main characters that affect stability. In addition to these, Brownian motion, diffusion, osmotic pressure, sedimentation, viscosity, surface tension, interfacial charge and electrical properties play a critical role for the formation of stable suspension in colloidal systems. Performance of the suspensions can be improved by understanding the effect of colloidal behaviors on such properties as viscosity, settling and effective size (Trefalt & Borkovic, 2014). Derjarguin, Landau, Verwey, and Overbeek (DLVO) improved a theory of colloidal stability, which gives information about interactions between colloidal particles and their aggregation behaviors (Matthews & Rhodes, 1970). Surface forces at the interface of the particle and the liquid are very important for the colloids. One of the major surface effects is the *electrokinetic effect*. Each colloid possesses "like" an electrical charge that produces repulsive and van der Waals (attractive) forces. According to the DLVO theory, agglomeration and stability of particles are determined by attractive and repulsive forces between individual particles (Hiemenz & Rajagopalan, 1997). The particles attract each other due to van der Waals force and the colloids steadily agglomerate. This agglomeration causes to change of characteristic properties of suspensions (Kulkarni et al, 2003). The interaction of the electrical double layer surrounding each particle is called electrostatic repulsive force (Ohshima, 2014). Electrostatic stability is provided with the balance between the attractive and repulsive forces acting on the charge of particles. They are depicted in Figure 2.5.

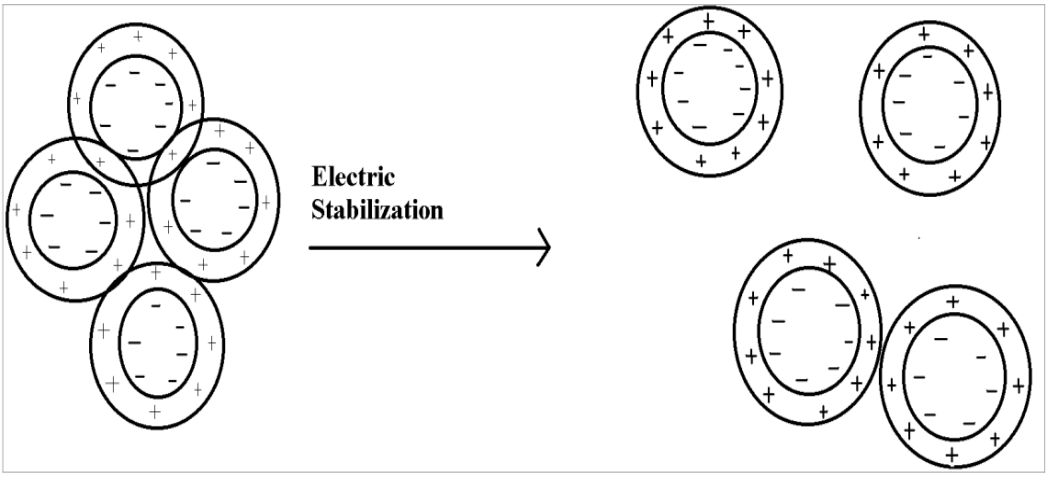

Figure 2.5: Electrostatic stabilization in a suspension (Hunter, 1981).

Steric stability is maintained by changing liquid's pH and/or the ionic species in solution and completely covering the particle by a polymer. The effective steric stability method is applied by covering the particle surface by a polymer. It is shown in Figure 2.6. The amount of polymer should be enough to cover each particle surfaces but not more that. If the amount of polymer is too much, residual polymers cause the flocculation either by van der Waals attractions between the residual polymer or by bridging. The polymer is adsorbed on two or more particles, simultaneously (Tadros, 2014).

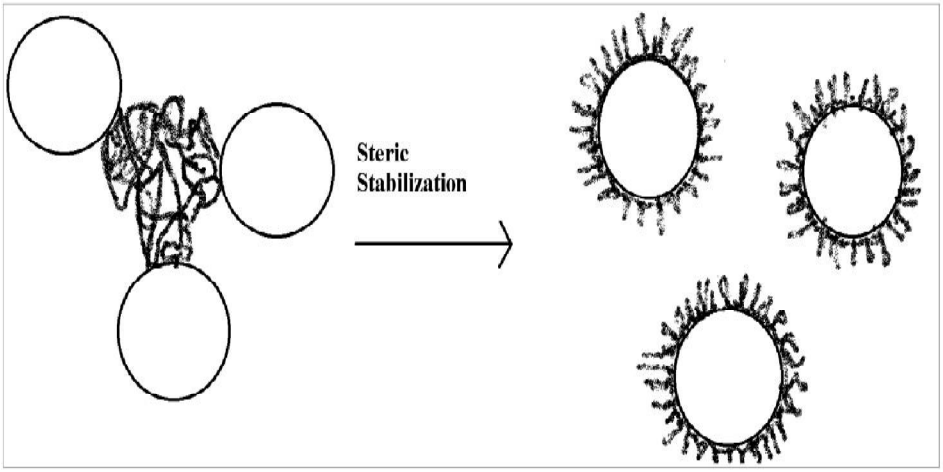

Figure 2.6: Steric stabilization in suspension (Hunter, 1981).

2.3 Rheology and Electrokinetical Properties

2.3.1 Rheology

2.3.1.1 Flow models

Flow behavior is described according to the relationship between shear stress and shear rate (Luckham & Rossi, 1999). Newton's Law states that when a force "F" is applied to first layer of two boundary layers with a surface area of "A" (apart with a distance of "dy") while the second layer is kept stationary, the velocity of the first layer will increase an amount of "dv" (Russel et al, 1989). They are depicted in Figure 2.7. According to this information, the ratio of force to the area is identified as shear stress and its unit is Pascal (Pa). Consequently, the shear rate is described as the ratio of "dv/dy" and its unit is s^{-1} (Israelachvili, 2011).

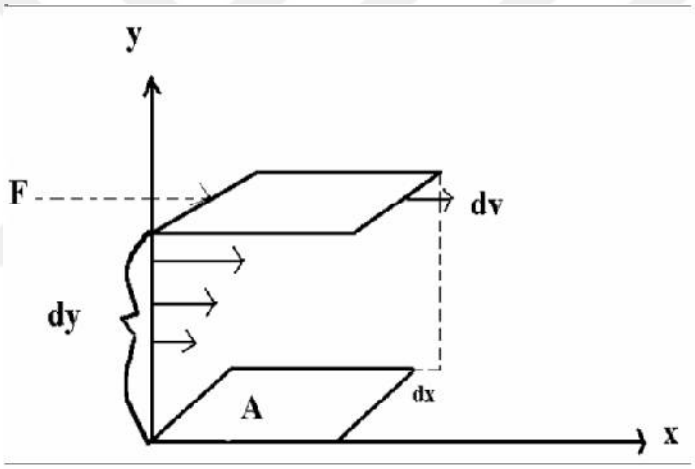

Figure 2.7: Newton's Law of flow behavior (Israelachvili, 2011).

Viscosity is described as the resistance of a fluid to flow of and also as the ratio. The plot of shear stress versus shear rate is called a consistency curve. Figure 2.8 shows that shear stress directly comparative to the shear rate. This type of flow is called Newtonian flow and for such flow viscosity is constant. The mathematical expressions for Newtonian fluids are given below:

$$\text{Shear stress: } \tau = F/A, \tag{2.1}$$

$$\text{Shear rate: } \gamma = dv/dy, \tag{2.2}$$

$$F/A = \eta \, . \, dv/dy, \tag{2.3}$$

$$\tau = \eta \, . \, \gamma \tag{2.4}$$

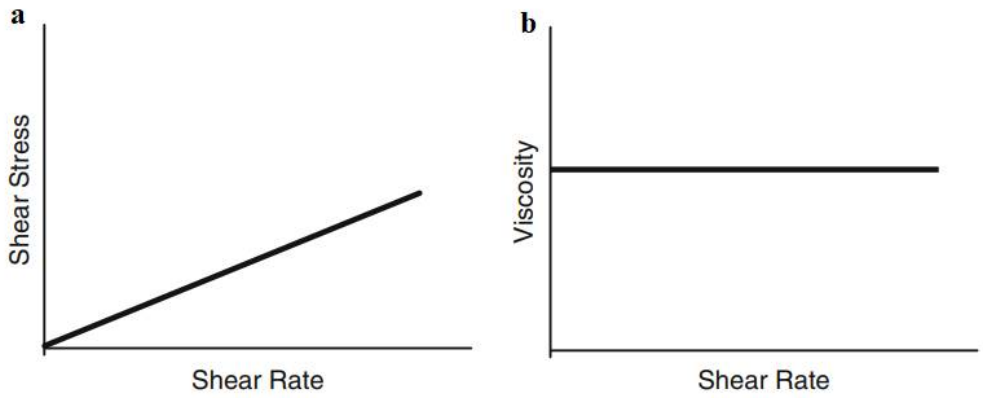

Figure 2.8: Flow behavior (a) and viscosity (b) according to Newton's Law (Tadros, 2010).

On the other hand, Non-Newtonian fluids do not obey the Newton's Law. Non-interacting or weakly interacting particles show Newtonian flow and constant viscosity. In Non-Newtonian fluids, particles interact or deform each other and their viscosities resist to changing shear rate (Bekaroglu et al, 2017). Viscosity measurement is sufficient to determine the Newtonian or Non-Newtonian fluids. In the literature, the common Non-Newtonian flow types are Pseudoplastic, Bingham plastic, dilatant, and Bingham ideal plastic. They are shown in Figure 2.9. Their viscosity varies with the shear rate as illustrated in Figure 2.10 (Luckham & Rossi, 1999).

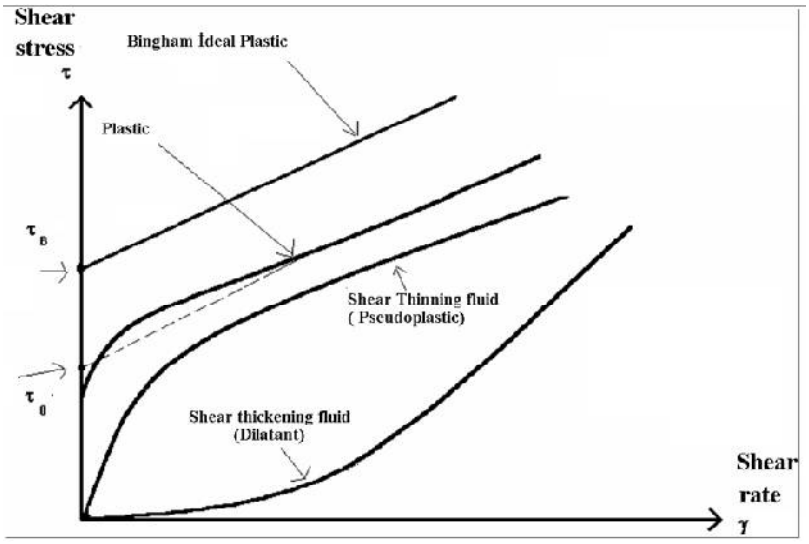

Figure 2.9: Non-Newtonian flow behaviors (Israelachvili, 2011).

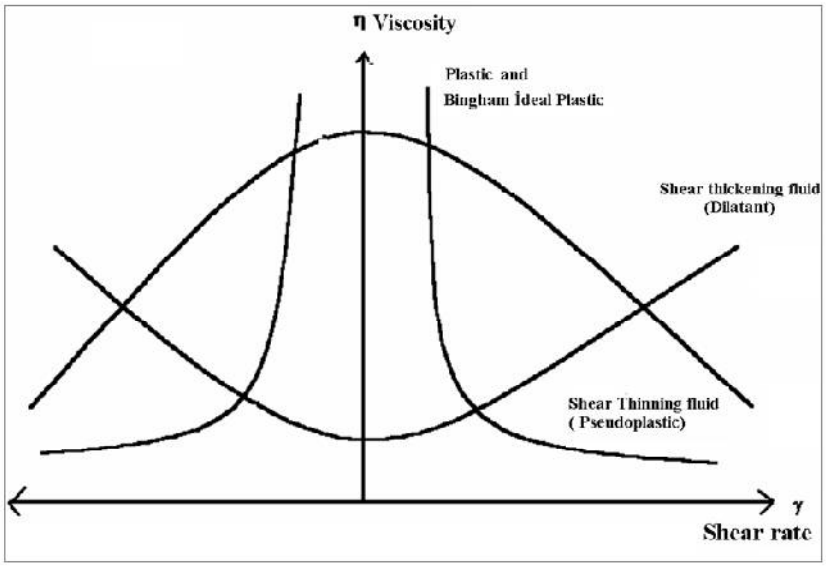

Figure 2.10: Viscosity-shear rate graphs of Non-Newtonian fluids (Israelachvili, 2011).

2.3.2 Electrokinetical properties

2.3.2.1 The electrical double layer

The electrical double layer model is used to understand how electrical repulsive force occurs in between charged colloids and their ionic environment.

Firstly, counter ions, which are positive ions, are attracted to the negative colloid surfaces and formed a layer. This layer's name is the Stern layer. Additional counter ions are attracted to the negative colloid and they fully cover the negative colloid surface. Continuous addition of counter ions cause repulsion. The second layer, which is form by counterions, is called the diffuse layer. When the number of counter ions increases on the surface, the distance of the surface on the negative colloid decrease. This process continues until reach equilibrium with the counterion concentration in the solution (McBride, 1997).

The diffuse layer can be stated as a charged atmosphere on the colloid surface. The charge density at any distance from the surface is equal to the difference in concentration of positive and negative ions at that point. Charge density near to colloids reduces gently until zero with distance because positive ions and the negative surface of colloids balance each other. They are depicted in Figure 2.11 (Zeta-Meter, Inc., Staunton, VA).

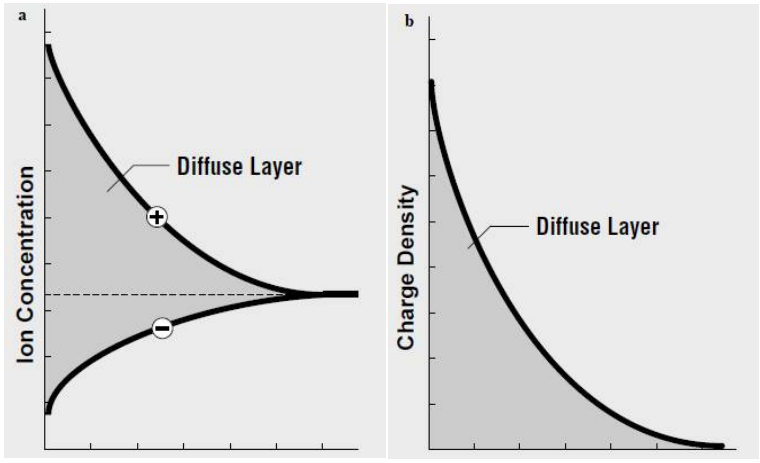

Figure 2.11: (a) Variations positive and negative ion concentration on the negative colloid surface and (b) the difference in negative and positive charge density - net effect.

2.3.2.2 Zeta potential

When an electric field is applied across the dispersion, charged particles in the dispersion will move toward the electrode of opposite polarity. This is called electrophoresis. Undergoing electrophoresis, if a laser beam is passed through the sample, moving particles scatter lights and change frequency. The electrophoresis mobility (U; $m^2V^{-1}s^{-1}$) can be determined by measuring the frequency shift and considering the laser wavelength and scattering angle (Jiang et al, 2008). Zeta potential can be calculated from electrophoresis mobility by using Smoluchowski equation:

$$\zeta = \mu U/\varepsilon \qquad (2.5)$$

where ε is the electric permittivity of the medium ($C^2N^{-1}m^{-2}$).

The double layer is formed to neutralize the charged colloid. Negative colloid and their surrounding liquid possess the electrokinetic potentials. Differences in these potentials form surface potential. The magnitude of surface potential depends on the surface charge and thickness of the electrical double layer (Hunter, 1981).

The particle's mobility is related to the dielectric constant and viscosity of the suspending liquid and to the electrical potential at the boundary between the moving particle and the liquid. This boundary is called the slip plane and that point where Stern layer and diffuse layer meet (Israelacvili, 2011).

As a result, surface potential is not zeta potential. Figure 2.12 shows that zeta potential is an electrical potential related to particle's mobility (Zeta-Meter, Inc., Staunton, VA).

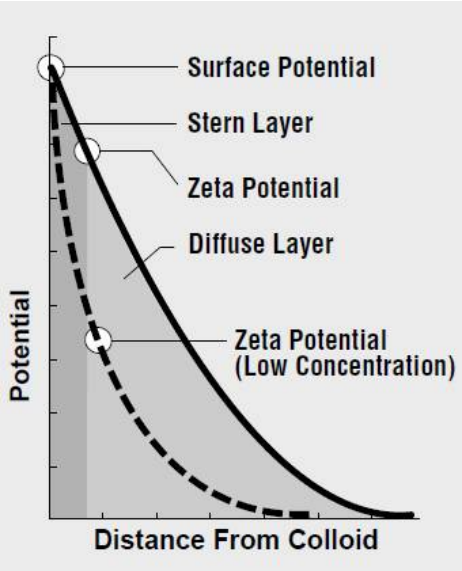

Figure 2.12: The relationship surface potential and zeta potential.

2.4 Biological Membranes and Liposomes

2.4.1 Biological membrane structure

In all cell types, there is a membrane to separate inside and outside. Membrane protects the cell against external influences such as harmful organisms or components. In addition, membranes of advanced organisms are divided to compartments according to their functions. The major components of cell membrane are phospholipids and proteins. They are also attached to carbohyrates to form glycophospholipids and glycoproteins (Weerd et al, 2015).

Phospholipids molecules are composed from head and tails groups. Head group have three components which are choline, phosphate and glycerol. These groups are attached to each other with chemical bonds. Tail groups include acyl hydrocarbon chains. Head group and tail groups are linked with ester bond. Head group attracts water and named as hydrophilic. Tail groups, on the other hand, repel water and named as hydrophobic. Phospholipid structure is illustrated in Figure 2.13.

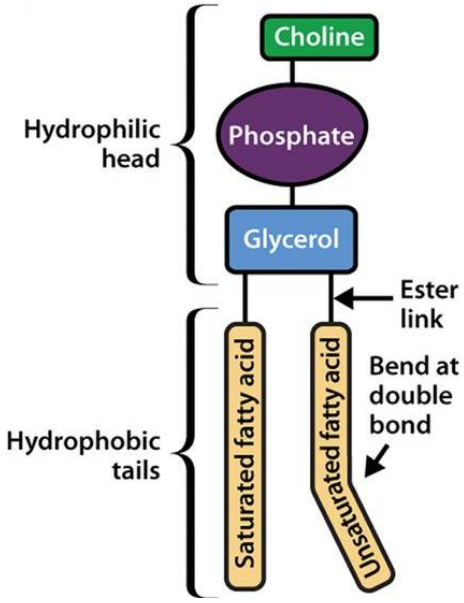

Figure 2.13 : Structure of phospholipid (Watson, 2015).

When phospholipids are introduced to aqueous solution, they form the most stable form via molecular interactions. This is affected by pH, salinity, and chemical nature in solution. Therefore, they can be bilayer or liposome structure (Nicolson, 2014).

There are many types of glycophopholipds and they are classified as anionic, cationic, pH sensitive or synthetic and natural. Phosphatidylcholine (PC) is a major components of cell membranes, and constitutes more than 50% in cell membrane. Phosphatidylethanolamine, phosphatidylserine (PS), phosphatidylinositol and phosphatidic acid are the other types of glycerophospholipids. They are shown in Figure 2.14.

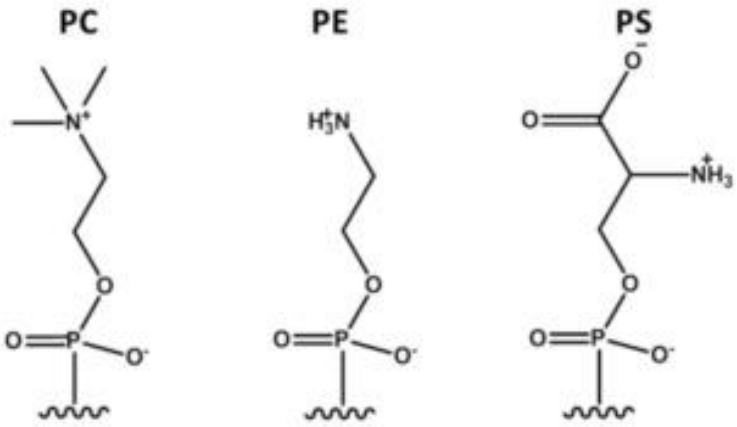

Figure 2.14: The chemical structure of various lipids (Henry et al, 2012).

2.4.2 Liposomes

Phospholipids possess both hydrophobic and hydrophilic groups. When phospholipids contact with aqueous solution, tail groups are attracted to each other with van der Waals forces and hydrophobic interactions and close the structure. Head groups, being hydrophilic, stay outside of the structure interacting with water, while tail groups not. The forming structure is a vesicular system called as liposome and shown in Figure 2.15. Water or aqueous solution is found both inside and around the liposomes.

Liposomes are classified according to their size and number of layers such as multi-, oligo-, or uni-lamellar. They are used in many areas because of their properties. Since they have both hydropilic and hydrophobic areas, they can be used to transport hydrophobic and hydrophilic drugs. Hydrophilic drugs can be entrapped inside of liposomes whereas hydrophobic ones are incorporated into the membrane and transported. Moreover, liposomes can be modified with ligands or polymers for different usage areas including targetting (Torchilin, 2005; Peetla et al, 2009).

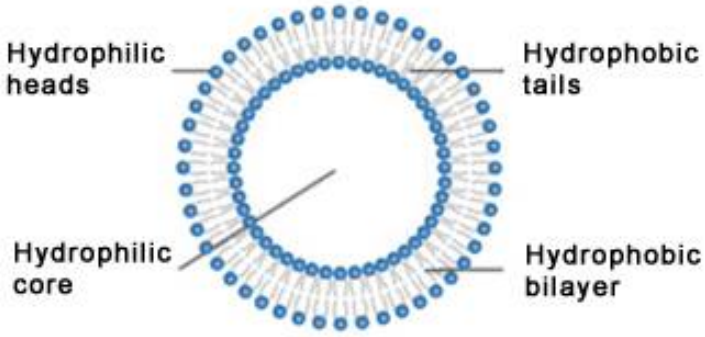

Figure 2.15: The structure of liposome (Url-1).

2.5 Quartz Crystal Microbalance with Dissipation (QCM-D)

QCM-D is a very sensitive, surface sensitive technique which allows in situ real-time, label-free evaluations of molecular interactions and gives information about viscoelastic or rigidity of adlayer materials (Yousefi et al, 2016). It can be used in many fields of biomedical, pharmaceutical, food, environment industry. Especially, it

is used to observe membrane-protein, protein-lipid, cell-cell, antigen-antibody interactions etc. (Kazanawa & Nam-Joon, 2009).

2.5.1 Basic principles of QCM-D

QCM is a system established on piezoelectric effect discovered by Curie brothers in 1880. It is used many fields of industry such as electric, biomedical, communication etc. (Qiao et al, 2016). Piezoelectricity means that electric produces with pressure or vice versa (Bradshaw, 2000). Application of AC field to the quartz, a piezoelectric material, cause expansion and contraction of the crystal.

QCM is a sensor to measure the changes of mass on the surface in the ranges of nanogram because of the piezoelectric effect. By this way, the amount of adsorbed or desorbed mass on the quartz crystal surface can be quantified.

Surface was designed as a circular piece of quartz between two metal electrodes like a sandwich model. This establishment was generally called AT-cut (Dixon, 2008). It provides stability against low-temperature coefficients and shear mode of oscillation It is shown in Figure 2.16.

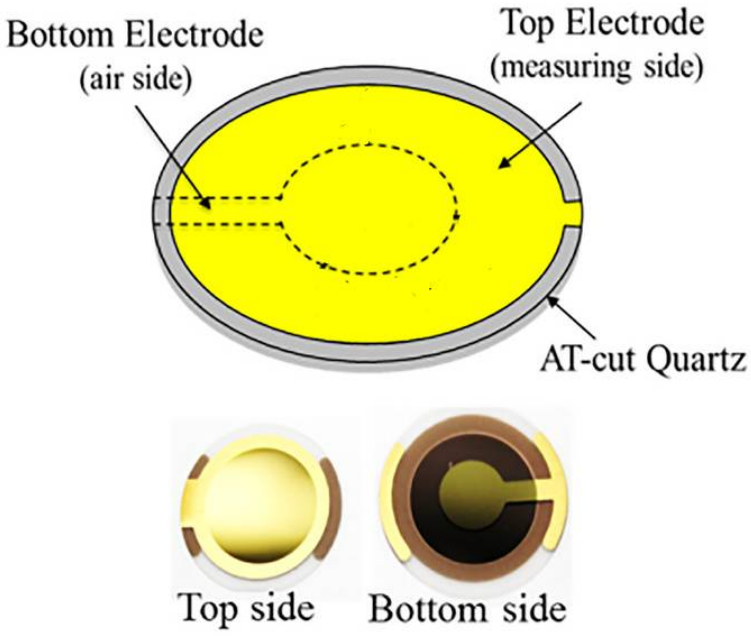

Figure 2.16: The schematic illustrations of AT-cut quartz crystal surface (Qiao et al, 2015).

The electrodes are connected to an oscillator and when AC voltage is applied to the electrodes, the crystal starts to oscillate with a defined resonance frequency. Addition

of mass to the surface, for example, causes to a decrease in the frequency. This alteration is founded by Sauerbrey (Rodahl et al, 1995). The mathematical expression of harmonic resonance by Sauerbrey;

$$\Delta m = -C(\Delta f_n/n) \tag{2.6}$$

where Δm is the adsorbed mass on the surface, C is the mass sensitivity constant (17.7 $ng \cdot cm^{-2} \cdot Hz^{-1}$ at f = 5 MHz), and Δfn is the change in the resonance frequency at the n^{th} harmonic (Rodahl et al, 1995). n is the harmonic order which has 1, 3, 5, 7, 9 and 11 values. C is a constant independent of the harmonic order n. According to Sauerbrey results frequency should be normalized with harmonic order and a constant value should be obtained for every harmony. There are three assumptions according to Sauerbrey (Cho et al, 2007).

1. The adsorbed mass must be small from the mass of quartz crystal.

2. The mass adsorbed leads to a rigid layer.

3. The mass adsorbed is distributed over the active area of the surface crystal.

There are deviations from Sauerbrey assumptions. First of all, mass adlayer may not be rigid but be viscoelastic. Frequency changes is very sensitive to mechanical properties such as shear modulus and viscosity. Secondly, dry mass can not be measured properly by QCM. Adsorbed materials are formed soft film on the surface, therefore they include water and vesicle adsorption also contain important amount of water (Cho et al, 2007).

2.5.2 The dissipation

The damping or dissipation is a property added to QCM later. It gives information about viscoelastic properties of adlayer film. D describes the energy lost during one oscillation cycle to whole energy stored in oscillator (Rodahl et al, 1995), the mathematical expression is,

$$D = E_{Dissipated} / 2\pi \times E_{stored} \tag{2.7}$$

Dissipation is affected by the size and flexibility of adsorbed molecules. If they increases, dissipation also increases.f is affected from adsorbed mass and when mass increases, f decreases. Changes of frequency and dissipation are measured

simultaneously by QCM-D. The illustrated QCM-D result by its software is presented in Figure 2.17 showing changes of frequency and dissipation with time. Properties of materials such as rigidity/viscoelastic or adsorption/desorption on the surface are determined with this type of plot. Figure 2.17 a shows that there are adsorbed mass on the surface but since it is rigid dissipation does not change much Figure 2.17 c to d shows the frequency and dissipation changes when more flexible layer is introduced to the surface.

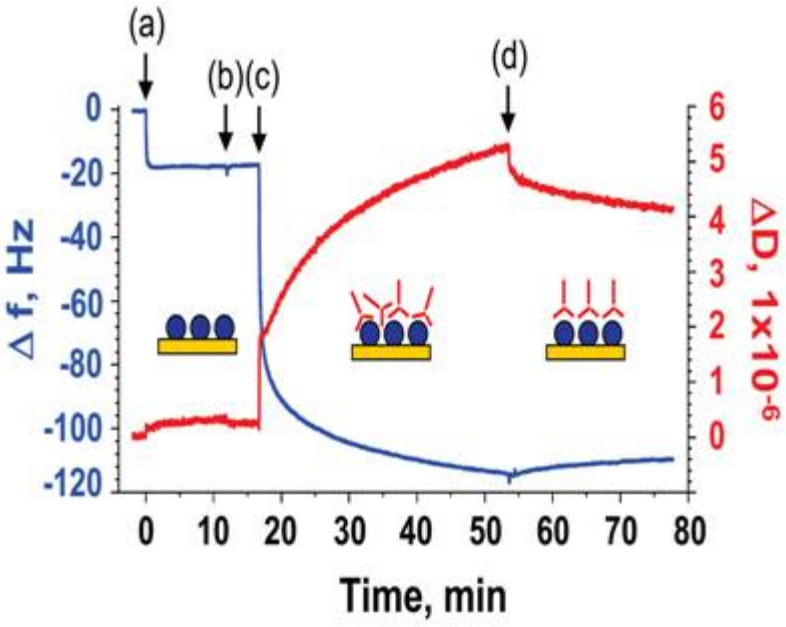

Figure 2.17: Example of raw data in QCM-D. Frequency changes are shown blue lines and dissipation changes are shown red lines (Dixon, 2008).

2.6 Polymers

Polymers are made of repeated units which are called monomer. They can be synthetic or natural. They are divided by thermoplastics, thermosets, elastomers and synthetic fibers, e.g. Nylons, poly(vinyl chloride) (PVC), polyethylene (PE) etc., however biopolymer or biological polymer is obtained from living organisms such as carbohydrates and proteins etc.

2.6.1 Poly(vinyl alcohol) (PVA)

PVA is a water soluble synthetic polymer with a simple chemical structure. The structure of PVA is shown in Figure 2.18. It has low environmental impact and high biodegradability and approved by FDA (The U.S. Food and Drug Administration) to

be used in close contact with food products. Consequently, PVA is used in many industrial areas such as textile industries, paper manufacturing, food packaging industries and fabrication of medical devices. Moreover, PVA is used a biomaterial due to its biocompatible, nontoxic, no carcinogenic, and bioadhesive characteristics (Tadavarthy et al, 1975).

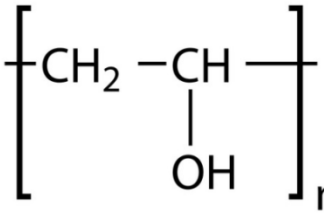

Figure 2.18: The chemical structure of PVA.

PVA is synthesized from vinyl alcohol monomer which is not stable in this form, however it rearranges to its tautomer, acetaldehyde (Kulkarni, 1966). Consequently, PVA is produced by the emulsion polymerization of vinyl acetate to poly(vinyl Acetate) (PVAc). This polymerization reaction is depicted in Figure 2.19.

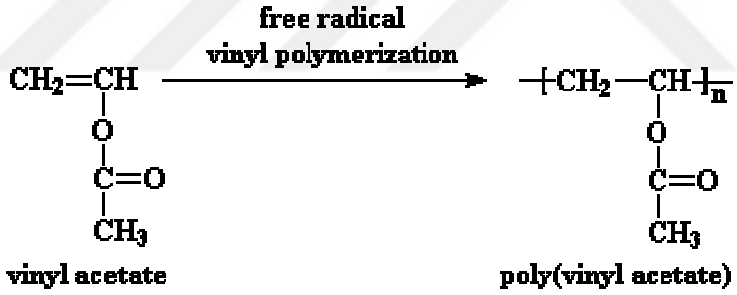

Figure 2.19: The polymerization process vinyl acetate to PVAc (Url-2).

Then, PVA is obtained from hydrolysis of poly(vinyl Acetate) (PVAc) with NaOH. The hydrolysis reaction is depicted in Figure 2.20.

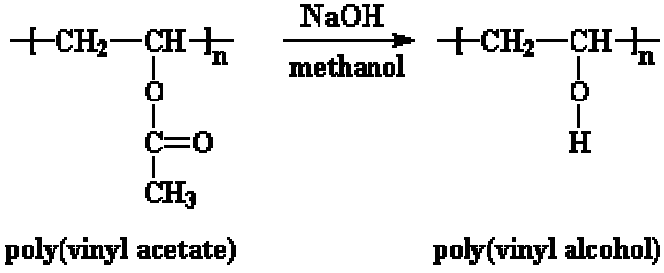

Figure 2.20: The hydrolysis process of PVAc to PVA (Url-3).

Supplied PVA grades have high degree of hydrolysis (above 98.5%). The degree of hydrolysis expresses the amount of acetate group of the polymer and it gives information about PVA such as solubility, chemical properties and crystallizability of PVA (Kurkamin, 1966).

The degree of hydrolysis and polymerization affect the solubility of PVA in water (Finch, 1973). High degree of hydrolysis causes low solubility in water. As shown in Figure 2.21.

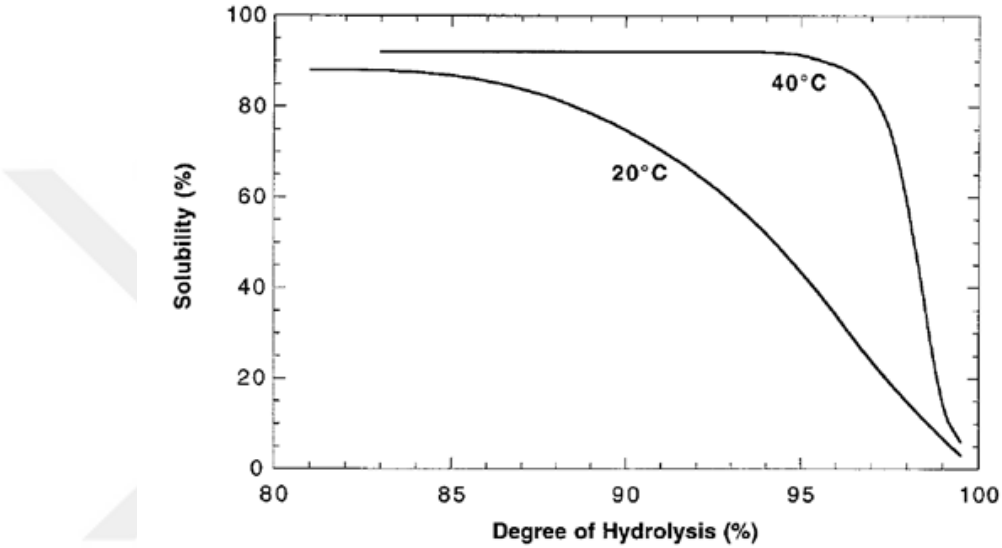

Figure 2.21: The percent solubility versus percent of degree of hydrolysis graph (Baker et al, 2012).

The molecular weight distribution affects characteristic properties of PVA including crystallization, adhesion, mechanical strength, and diffusivity. Commercial PVA has average molecular weight of M_n= 77.000 at dissolution temperatures of 20 and 40°C (Baker et al, 2012). Its 5% solution shows a pH in the range of 5.0 to 6.5. Melting point of PVA is between 180°C to 190°C (Eliassaf, 1972).

PVA is degradable polymer and is not toxic during degradation. De Merlis and Schoneker determined that PVA is safe to use in injected products in 2003. Its LD_{50} is recorded between 15 and 20 g/kg demonstrating low acute oral toxicity.

2.6.2 Chitosan

Chitosan is a natural polysaccharide obtained from chitin derived from shells of crustaceans such as crab, shrimp, lobster etc. (Elieh & Hamblin, 2016). Chitosan is obtained from chitin by deacetylation by enzymatic reactions or chemical processes.

Chemical process with acids or alkalis is preferred by producer due to its low cost and controllable mass production (No & Meyers, 1995). However, glycosidic bonds of chitin are very sensitive to acids; generally, alkali deacetylation is used to obtained chitosan from chitin (Younes & Rinaudo, 2015).

Chitin is reacted with NaOH solution to remove the protein parts, then fixed with HCI solution to demineralize and finally decolorized. Obtained chitin is treated 40-50 % alkali solution at 100-150°C and chitosan is obtained. Figure 2.22 shows manufacturing of chitosan from chitin with all details.

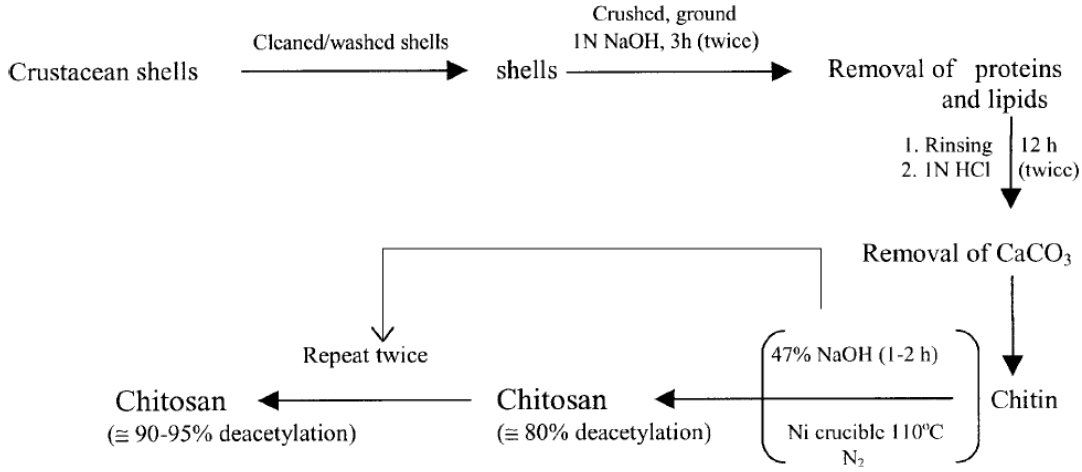

Figure 2.22: Manufacturing of chitosan from chitin (Singla & Chawla, 2001).

Chitosan has functional groups which are primary and secondary hydroxyl groups and amine group as repeated units on the structure. As shown in Figure 2.23. These functional groups are more chemically active than chitin. These reactive groups also provide the chemical modifications on chitosan structure. Therefore, mechanical and physical properties of chitosan are modifiable (Tan, 2009).

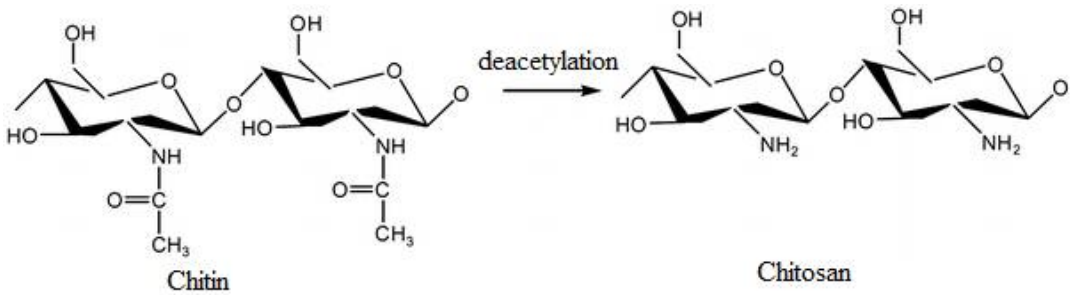

Figure 2.23: The deacetylation reaction from chitin to chitosan (Nilsen-Nygaard et al, 2015).

The degree of deacetylation (DA), molecular weight, water retention, viscosity, pKa, energy of hydration and crystallinity are also very important properties of chitosan (Atala et al, 2010). Molecular weight of chitosan can range between 300-1000 kDa and the degree of deacetylation can change from 30% and 95% depending on chitin source and preparation techniques.

Chitosan is affected by differences of pH conditions. For example, decreasing temperature and increasing the degree of deacetylation lead increased viscosity in acidic environment (Skaugrud, 1991). Also, chitosan is insoluble in alkaline and neutral solution (Singla & Chawla, 2001; Errington, 1993).

Chitosan is used in wide range of areas such as pharmaceutical and medical applications, paper production, textile, biotechnology, cosmetic, food processing etc. due to its biological, chemical and physical properties (Bashar, 2013 and Islam, 2017). Also, because of its biocompatibility, biodegradability, non-toxicity, and antimicrobial properties, it is preferred by biomedical engineering (Chou et al, 2015).

3. EXPERIMENTAL PART

3.1 Materials and Chemicals

Iron oxide (Fe_3O_4) nanoparticles (544884), chitosan from shrimp shells (Low viscosity, 50494), poly(vinyl Alcohol) (PVA) (363138), acetic acid (27225), potassium phosphate monobasic (P5379), sodium phosphate dibasic dihydrate (O4272), sodium chloride (134239), potassium chloride (P9541) were purchased from Sigma–Aldrich Co. and used without further any purification. Phosphatidylcholine (PC) (840051), L-α-phosphatidylserine (PS) (870336P), 1,2-dioleoyl-3-trimethylammonium-propane (DOTAP) (890895P) and liposome extrusion equipment (610000) were purchased from Avanti Polar Lipids. Chloroform was purchased from Merck. Distilled water was used every steps of experiments. Filters (SLGV033RS) with 0.2 µm pores were used to filter phosphate buffer saline (PBS, 0.01M pH 7.4), and all solutions were degassed before using at Quartz Crystal Microbalance with Dissipation (QCM-D).

3.2 Methods

3.2.1 Preparation of iron oxide nanoparticles (IOPs)

IOPs were purchased as powder and dispersed in distilled water. Concentrations of IOPs were prepared as 2% (w/v) according to literature (Bekaroglu et al, 2015). Dispersions were shaken overnight at room temperature and before measurements and coating with polymers; they were ultrasonicated for 5 min. The dispersion solutions can be stored at +4 °C for 4 months.

3.2.2 Synthesis of polymer coated IOPs

3.2.2.1 Preparation of PVA-coated IOPs (PVA-IOPs)

PVA was prepared with distilled water as 4 g/L stock concentration. Adsorption method was used to coat IOPs with biopolymers to have stable and fully covered

surfaces to obtain non-toxic, biocompatible, multifunctional magnetic particles. IOPs (2%) were treated with PVA in variable ranges of polymer concentration (between 0.1-1 g/L). The dispersions were shaken overnight at room temperature. Coating concentrations were determined according to colloidal stability by using zeta potential. PVA has ionizable groups so its charge changes from acidic to basic conditions. Therefore, PVA-coated IOPs were prepared at different pH values to observe changes in zeta potential, particle size, rheology and viscosity of obtained sample. NaOH (2M) and HCI (2M) were used to adjust the pH of the medium (4 and 10). Adjustment of pH was done after PVA was coated to IOPs surfaces. Physiological pH condition was provided with phosphate buffer saline (PBS, pH 7.4). PVA-coated IOPs were precipitated with external magnetic field and supernatant was changed with PBS.

3.2.2.2 Preparation of chitosan-coated IOPs (C-IOPs)

Chitosan was solved with acetic acid (1 M) at the concentration of 1.25 g/L. IOPs were coated with chitosan between the ranges of 10^{-5} to 1 g/L concentration. Zeta potential values were determined to select the colloidal stable concentrations of chitosan-coated IOPs. Then, determined concentrations were treated with acid, base and PBS at different pH values.

3.2.3 Preparation of liposomes

3.2.3.1 Preparation of stock solutions

Stock solutions of phosphatidylcholine (PC) (20 mg/mL), phosphatidylserine (PS) (10 mg/mL) and 1,2-dioleoyl-3-trimethylammonium-propane (DOTAP) (5 mg/mL) lipids were prepared separately by dissolving in chloroform solution at +4°C. Solutions were stored in -20°C as aliquots.

3.2.3.2 Preparation of liposomes

PC, PS, and DOTAP at different concentrations (20 mg/mL, 2.5 mg/mL and 5 mg/mL, respectively) were dissolved in chloroform at +4°C and stored -20°C. To prepare liposomes, firstly, a thin lipid layer was formed. For this, PC solution was poured into a round bottom flask (200 µL) and the flask was rotated manually for evaporation of chlorofom. After the evaporation, dry nitrogen stream was used to

remove chloroform residues. Then 1 mL PBS (0.01 mM, pH 7.4) was added into flask and vortexed until homogenous solution was obtained. For the formation of small unilamellar vesicles from the obtained multilamellar vesicles, an extruder was used. For this, 1 mL of solution was passed through an extruder system that contain a polycarbonate membrane (100 nm pore size) with two syringe in both sides at least 21 times. Finally, the obtained solution was put into a falcon tube and diluted with PBS until last concentration of liposomes is 1 mg/mL. It can be stored +4°C during one week. By this method, 25% PS:PC and 25% DOTAP:PC liposomes were prepared.

3.2.4 Quartz crystal microbalance with dissipation monitoring (QCM-D)

QCM-D measurements were performed with QCM-Z500 (KSV Instrument) in a flow-through cell. It is shown in Figure 3.1. A peristaltic pump and tubing (Tygon, R3607, ID:1.09 mm, wall thickness: 0.86 mm) were used to transport analyte solutions to the quartz crystal surface. All measurements were performed at 25°C. The measurement were performed at several harmonics (n= 3, 5, 7, 9 and 11) but all presented QCM-D data were recorded at the 3th harmonic and frequency shifts were normalized by division with 3. Prior to analysis, gold coated QCM-D sensors were treated in UV ozone for 15 min.

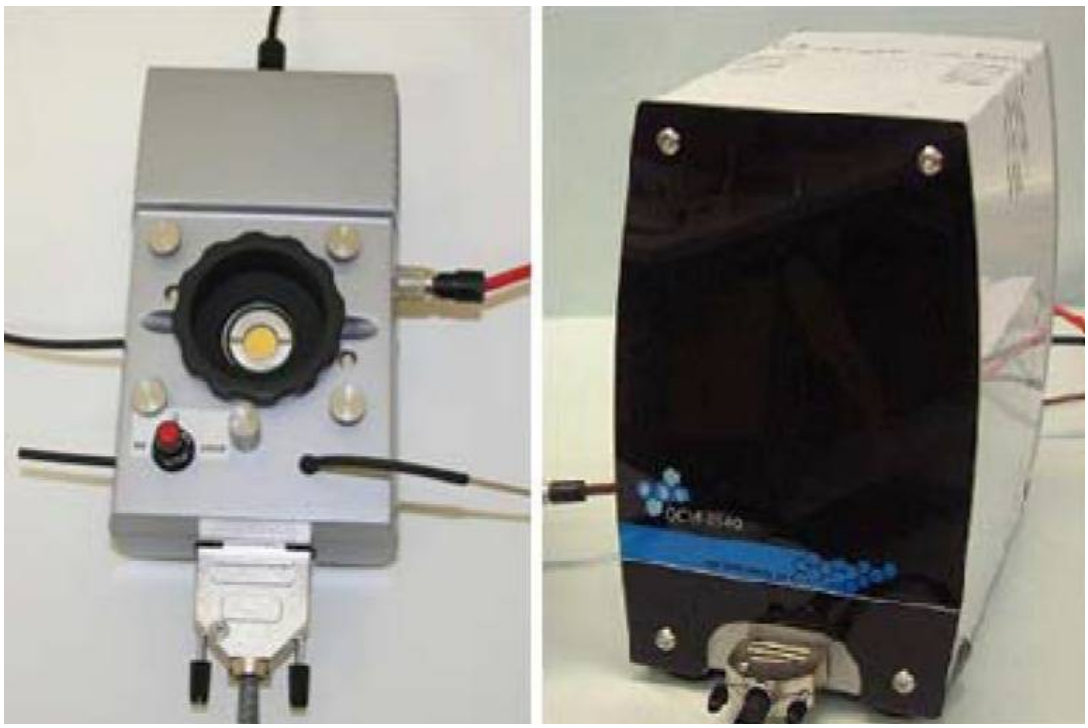

Figure 3.1: The QCM-D and electric unit.

3.2.5 Construction of lipid layer on QCM-D

In the QCM-D experiments, liposomes were added to clean gold surface. After the lipid layer formation as shown in Figure 3.2, PBS was passed through the flow chamber to remove unbound liposomes on gold surface. The Q-Tools data evaluation software (Biolin Scientific, Sweden) was used to estimate the mass adsorbed in different experiments. Presented calculated changes of frequency and dissipation were based on three experiments.

Figure 3.2: The formation of liposome on the gold surface.

4. RESULTS and DISCUSSIONS

4.1 Properties of Iron Oxide Nanoparticles (IOPs)

4.1.1 Electrokinetical properties of IOPs

Surface charges are effective on the stability of the nanoparticles dispersion. The surface charges also affect the cell membrane depending on the charge distribution of the particles and the membrane surface. Besides, if the particles make clusters, they can reduce the blood flow in the vessels. The plasma and blood cells constantly had a negative charge; IOPs with negative surface charge can minimize nonspecific contact with these components because of the electrostatic repulsions (Nosrati et al, 2018).

The zeta potential measurements were carried out using a Zetasizer 2000, Malvern Inst. All the dispersions were diluted with solvents such as water or PBS and ultrasonicated for 5 min. before the measurements.

IOPs were dispersed in distilled water as 2% concentration. pH of this dispersion was measured with pH paper and observed as 5. Zeta potential of IOPs was determined as -12.3 mV.

Addition any compounds onto the dispersion can change their colloidal properties. Therefore, the effect of the pH conditions on the colloidal particals were investigated at different pH values.

The pH value of the IOPs in water was measured as pH 5. HCI was added into the dispersion to prepared acidic condition (pH 3.5 and 4) and NaOH was added into the dispersion to prepared basic condition (pH 10). The neutral dispersion (pH 7.4) were prepared with magnetic decantation using PBS (0.01 mM).

Table 4.1 shows the zeta potential values of 2% IOPs dispersions different pH conditions. Zeta potential values of all samples indicates that all the dispersions, except pH 10, were unstable and showed aggregation.

Table 4.1: Zeta potential (mV) values of 2% IOPs in different pH conditions.

	pH 3.5	pH 4	pH 5	pH 7.4	pH 10
2% IOPs	32±1.7	39±2.2	-12.3±1.7	-17±0.2	-32±3.2

4.1.2 Rheological properties of IOPs

The flow properties of the IOPs dispersions were determined at different pH values by DVIII + type low-shear viscometer. Shear Stress(τ) and viscosity values were measured at changing shear rate from 0 s^{-1} to 330 s^{-1}.

Flow curves can be used to determine the interactions between the particles. The non-interacting or very weakly interacting particles mostly show Newtonian flows, which has a constant viscosity and a linear change between shear stress and shear rate. If the deforming of the material changes the arrangement of its microstructure and causes to increase the resistance to flow with any increase in shear rate, this kind of flow is called as shear thickening (Dilatant) flow behavior.

IOPs dispersion showed shear thickening flow behavior and plastic behavior at high shear rate values in Figure 4.1. The plastic flow can be found from the slope of the linear part of the curve at high shear rate area. The formed floccules were broken by the high shear. Dilatant and plastic flow are common between high suspension and tendency to flocculation solutions (Shaw et al, 1970).

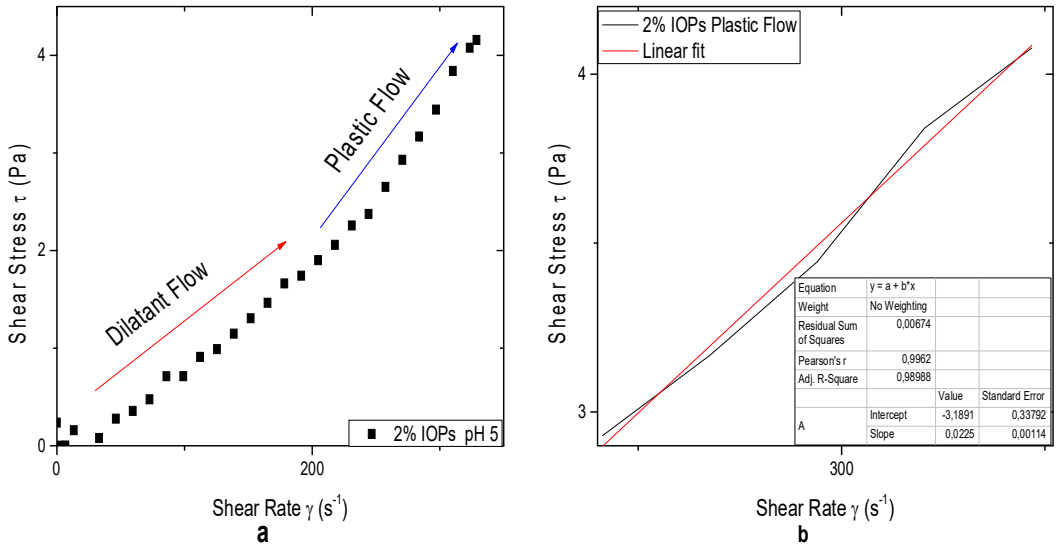

Figure 4.1: (a) Shear rate-shear stress graph and (b) plastic flow curve and linear fit of IOPs.

The flow type of the IOPs are determined as shear thickening flow. It is shown in Figure 4.2.

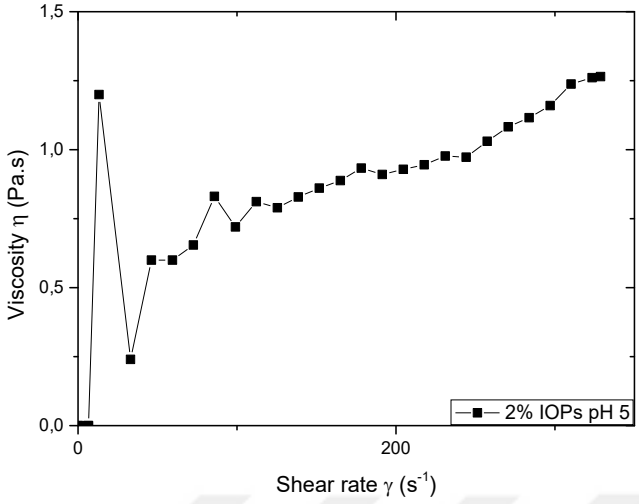

Figure 4.2: Viscosity-shear rate graphs of IOPs dispersion.

The flow behavior of the dispersion did not show any change under the different pH conditions. This situation is shown in Figure 4.3.

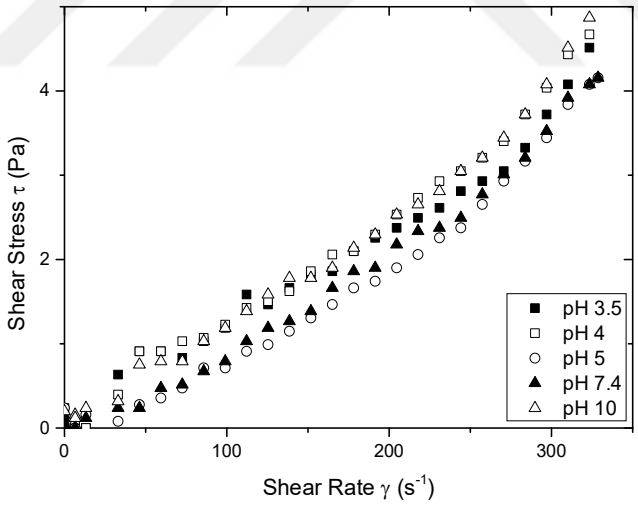

Figure 4.3: Flow curves of IOPs in different pH conditions.

The high shear rates can broke the interactions of the flocs of the particles, and can be resulted in a linear section on the flow curve. This area is called plastic flow. The IOPs showed plastic flow at high shear rates. The slope of the lineer part gives an average viscosity of that part which is called as plastic viscosity. In Table 4.2, the plastic viscosity values of the dispersions were given at different pH conditions.

Table 4.2: List of slope of plastic flow of different pH values.

pH	IOPs Plastic Flow slope
3.5	2.78 ± 0.114
4	2.34 ± 0.151
5	2.25 ± 0.114
7.4	1.75 ± 0.092
10	2.57 ± 0.132

Apparent viscosity is defined as the viscosity values at a specific shear rate. The apparent viscosity of the dispersions were given at Table 4.3 to compare the resistivity of the dispersions according to the different pH conditions.

Table 4.3: Initial and final shear rate (s^{-1})-viscosity (Pa.s) values of IOPs in different pH conditions.

IOPs	6.6 s^{-1}	323.4 s^{-1}
pH 3.5	0	1.39
pH 4	0.59	1.44
pH 5	0	1.26
pH 7.4	0	1.26
pH 10	2.39	1.50

4.1.3. Particle size (DLS) properties of IOPs

Particle size of the dispersion was determined by Malvern Inst. The dispersions were diluted with 1000 times dilution then all samples were ultrasonicated.

Acidic and basic conditions can change the state of the IOPs dispersions. Table 4.4 indicates that IOPs in pH 3.5 and pH 10 did not change their particle sizes. As a results, excessive acidic and basic medium did not affect the interaction of particles. In pH 7.4 and pH 4 conditions were caused by reduced interaction between particles. Consequently, particle sizes of these pH levels are smaller than others.

Table 4.4: Average particle sizes (d.nm) of IOPs in different pH conditions

	pH 3.5	pH 4	pH 5	pH 7.4	pH 10
IOPs	700	120	700	200	700

4.1.4 Fourier transform infrared spectroscopy (FTIR) properties of IOPs

FTIR spectrum analysis were examined in absorbance modes using Perkin Elmer Spectrum One Spectrophotometer. Its wavelenght range is 400-4000 cm^{-1} IOPs solution was dried in owen. KBr pellets with a concentration of 1% film were prepared for the measurements. The pellets were compressed under almost 10 tons for about 2 min.

The characteristic Fe-O stretching was observed at 583 cm-1. It is shown in Figure 4.4.

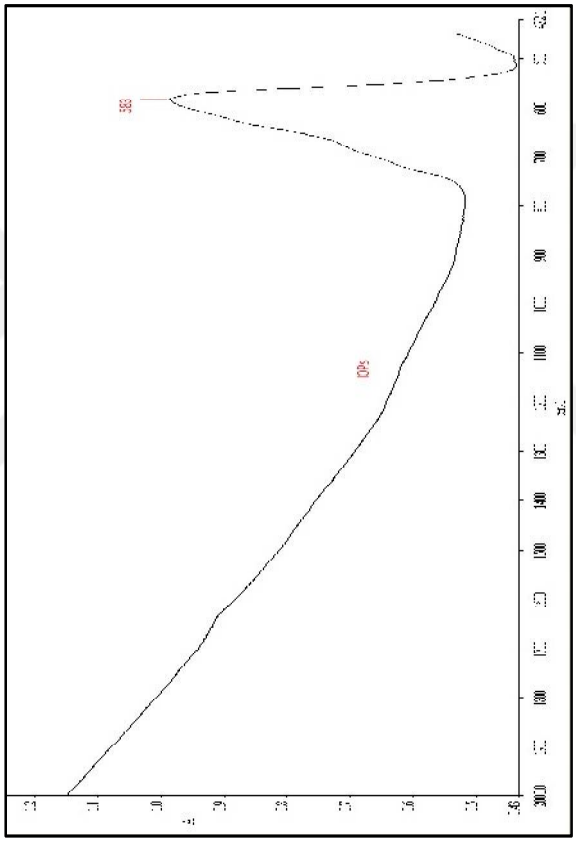

Figure 4.4: FTIR spectrum of IOPs.

4.2 Interactions with Poly(vinyl Alcohol) (PVA) and IOPs

In this part, IOPs were treated with PVA polymer to have stable and fully covered surfaces of IOPs by controlling the colloidal properties for the drug delivery applications. The interactions of the PVA and IOPs were determined by following the flow properties of the system, the zeta potential values, binding informations and particle size with different polymer concentrations and pH conditions.

4.2.1 Electrokinetical properties of PVA-coated IOPs (PVA-IOPs)

Zeta potential measurements brings details about the stability, or flocculation of the dispersions. It is a fundamental parameter which is a measure of the magnitude of the charge repulsion or attraction between particles (Tadros, 2007). The dispersion with zeta potential values in between -25 and 25 mV mostly show aggregation or flocculation (Isci et al, 2017). The zeta potential value of the IOPs dispersion in the absence of PVA was measured to be -12.3 mV which indicates that the dispersion is unstable and in aggregating regime. Adding PVA to the IOPs dispersion decreased the absolute value of the zeta potential values. Uncharged PVA polymer attached to the negatively charged surfaces of IOPs by the steric interactions and decreased the zeta potential values due to the bridging flocculation. Increasing concentrations of PVA caused to steric repulsions between PVA polymers and resulted a slight dispersive effect as a result of the osmotic effect of polymers. Further concentrations of PVA resulted in the whole coverage surfaces of the IOPs with PVA polymer and isoelectric point of the charge obtained from the dispersions. Isoelectric point of the charge also can cause to the flocculation but the steric interaction between the polymer enveloped surfaces of the IOPs prevented the flocculation.The surfaces of the IOPs fully covered sterically, and stable dispersions of particles obtained with 0.5 and 1.0 g/L PVA. As seen in Figure 4.5.

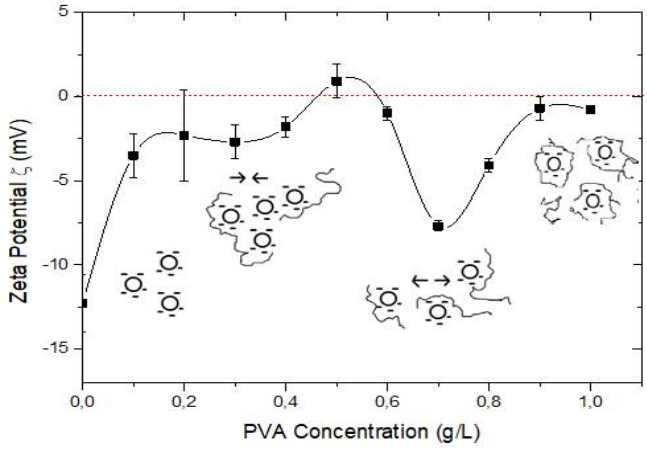

Figure 4.5: Zeta potential values of different PVA concentration coated IOPs.

According to the zeta results, other measurements such as particle size and rheological measurements were done for both 0.5 g/L PVA-IOPs and 1.0 g/L PVA-IOPs. These two samples were also examined in different pH conditions.

Table 4.5 shows that PVA-coated IOPs form flocculation in acidic and basic conditions. Particles are not stable in these conditions according to the zeta potential values.

Table 4.5: Zeta potential (mV) values of different pH conditions of PVA-coated IOPs.

	pH 4	**pH 5**	**pH 7.4**	**pH 10**
0.5 g/L PVA-IOPs	16.6± 0.8	0.9±1	0.6±1.1	-10.7±0.9
1.0 g/L PVA-IOPs	23.7±5.1	-0.8±0.1	2.4±0.6	-9.9±2.1

4.2.2 Rheological properties of PVA-IOPs

IOPs dispersion showed shear thickening flow behavior but the addition of PVA reduced the interactions because of a rearrangement of IOPs. The flow regime of IOPs changed into the Newtonian flow with PVA addition. The flow curves were given in Figure 4.6. Flow curve of 0.5 g/L PVA coated iron oxide nanoparticles were determined as nearly Newtonian flow compared to 1.0 g/L PVA-IOPs and IOPs.

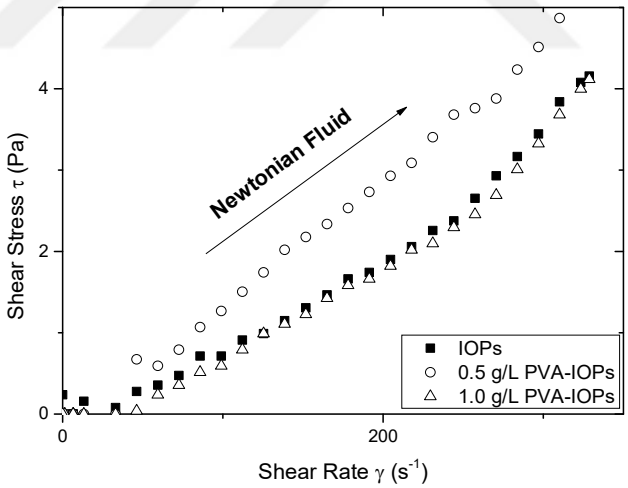

Figure 4.6: Flow curves of PVA-coated and uncoated IOPs.

According to the flow results, 0.5 g/L PVA reduced the interaction between particles and showed Newtonian flow in Figure 4.6. However, different pH conditions showed dilatant flows consequently they caused to increased interaction of particles and form flocculation as seen in Figure 4.7 a. 1.0 g/L PVA-IOPs show dilatant flow in Figure 4.7 b and changing of the pH condition did not change the flow type of the dispersion.

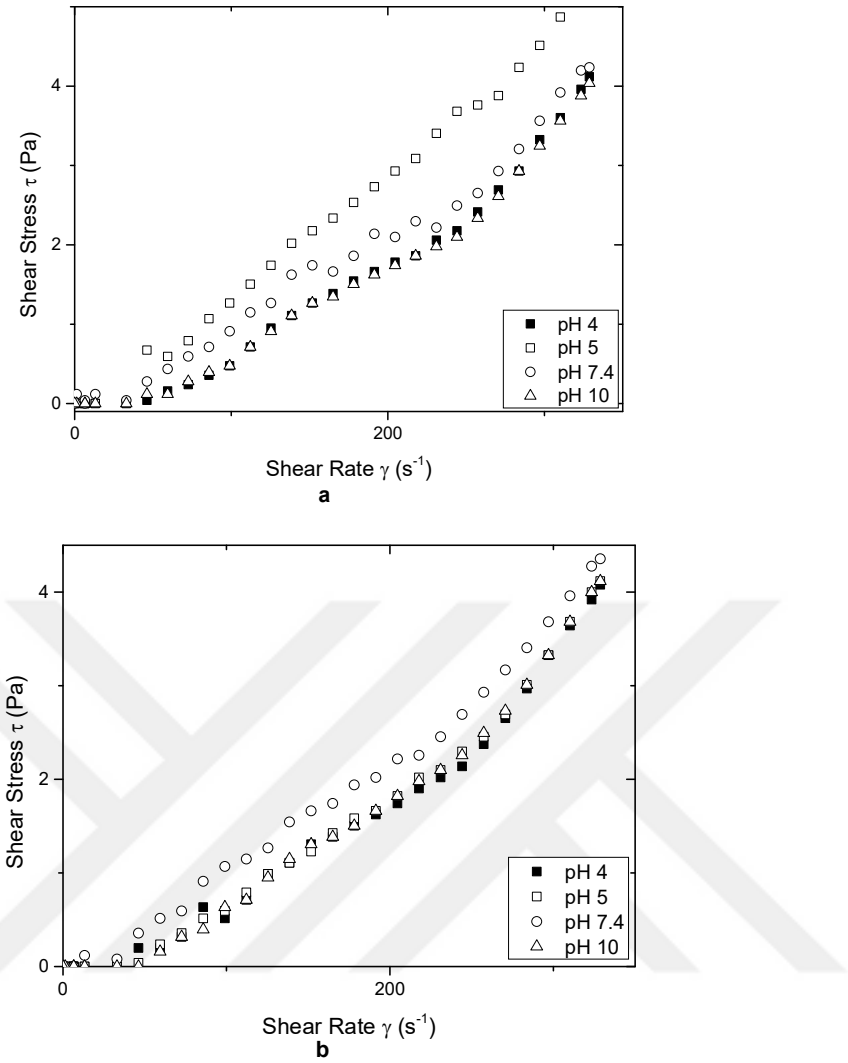

Figure 4.7: Flow curve of different pH levels (a) 0.5 g/L PVA-IOPs and (b) 1.0 g/L PVA-IOPs.

Plastic viscosity values were obtained from the slopes of 0.5 g/L PVA-coated IOPs flow curves. The plastic viscosity values were observed similar values in different mediums and these values were given in Table 4.6.

Table 4.6: Slopes of plastic flow of 0.5 g/L and 1.0 g/L PVA-IOPs in different conditions.

pH	0.5 g/L PVA-IOPs Plastic Flow slopes
4	2.47 ± 0.076
5	2.51 ± 0.05
7.4	2.45 ± 0.06
10	2.31 ± 0.04

Table 4.6 (continued): Slopes of plastic flow of 0.5 g/L and 1.0 g/L PVA-IOPs in different conditions.

pH	1.0 g/L PVA-IOP Plastic Flow slopes
4	2.42 ± 0.05
5	2.48 ± 0.02
7.4	2.1 ± 0.05
10	2.42 ± 0.05

All pH conditions except pH 7.4 were increased viscosity values. Consequently, they increased the interactions of particles, and they formed flocculations when IOPs were covered with 0.5 g/L PVA. In pH 7.4, final viscosity value was decreased compared initial value. As a result, 0.5 g/L PVA reduced to the interaction of particles and prevented agglomeration in pH 7.4. 1.0 g/L PVA was covered whole IOPs surfaces compared to 0.5 g/L PVA. Therefore, different pH conditions did not remarkably change viscosity final values as seen in Table 4.7.

Table 4.7: Initial and final shear rate (s^{-1})-viscosity (Pa.s) values of PVA-coated IOPs in different pH conditions.

0.5 g/L PVA-IOPs	**1.32 s^{-1}**	**328.6 s^{-1}**
pH 4	0	1.25
pH 5	0	1.61
pH 7.4	8.99	1.28
pH 10	0	1.22
1.0 g/L PVA-IOPs	**1.32 s^{-1}**	**328.6 s^{-1}**
pH 4	0	1.24
pH 5	0	1.25
pH 7.4	0	1.32
pH 10	0	1.25

4.2.3 Particle size (DLS) properties of PVA-IOPs

IOPs tend to agglomeration and formed flocculation in different particle sizes at changing pH conditions. 0.5 g/L PVA covered to the flocs surfaces and increased the particle sizes. However, 1.0 g/L PVA caused two different situations. 1.0 g/L PVA covered whole flocs surfaces and increased the particle sizes. Also, 1.0 g/L PVA reduced the interactions of IOPs and decreased the particle sizes. pH 7.4 caused to agglomeration of PVA-coated IOPs compared of IOPs sizes. Basic conditions decreased the interaction of PVA-coated particles and reduced to particle sizes. Acidic conditions showed different results to 0.5 g/L and 1.0 g/L PVA-IOPs. 0.5 g/L

PVA decreased the interaction of IOPs, therefore reduced the particle sizes in contrast to 1.0 g/L PVA as seen in Table 4.8.

Table 4.8: Average particle sizes (d.nm) PVA-coated and uncoated IOPs in changing pH levels.

	pH 4	**pH 5**	**pH 7.4**	**pH 10**
IOPs	120	700	200	700
0.5 g/L PVA-IOPs	130	800	500	150
1.0 g/L PVA-IOPs	500	140, 900	400	300

4.2.4 FTIR properties of PVA-IOPs

Characteristic Fe-O stretching vibration peak was determined at 583 cm^{-1} for Fe_3O_4. The results showed that addition of the polymer PVA did not change the spectrum of Fe_3O_4 as seen in Figure 4.8. The polymer addition was too low, so the characteristic peaks of the PVA did not appear on the spectrum.

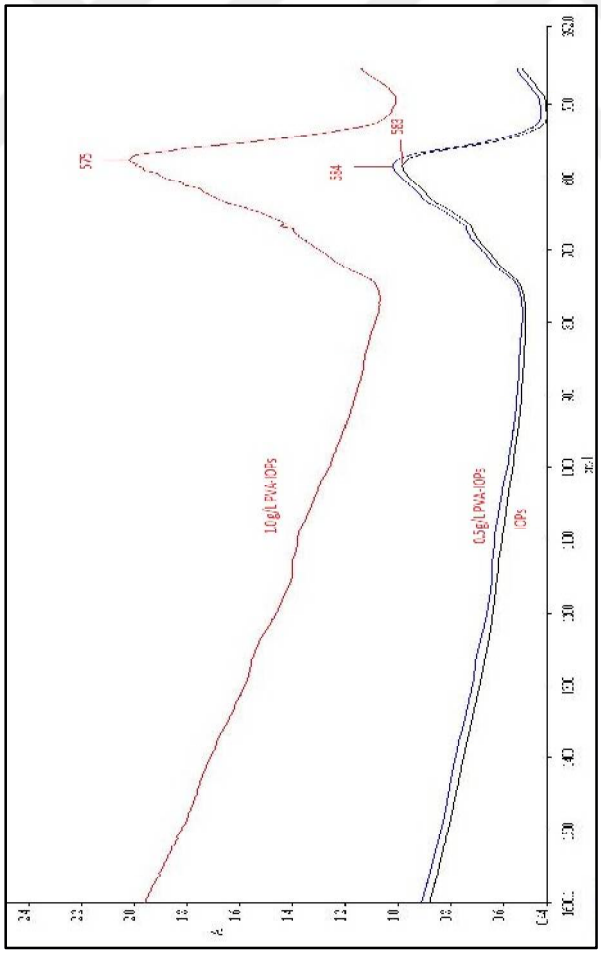

Figure 4.8: FTIR spectrum of PVA-coated and uncoated IOPs.

4.3 Interactions with Chitosan-Coated Iron Oxide Nanoparticles (C-IOPs)

4.3.1 Electrokinetical properties of C-IOPs

The effects of different concentrations of chitosan on IOPs was determined by electrokinetical properties. Samples were diluted and ultrasonicated before measurements.

Concentration of chitosan solution was prepared between 0.1 and 1.0 g/L chitosan-coated IOPs.

The zeta potential values of dipersion can give an idea about the colloidal stability of the dispersions. Positively chitosan polymer attached to the negatively charged surfaces of IOPs by electrostatic interactions and changed the zeta potential values to the positively charged surfaces as seen in Figure 4.9.

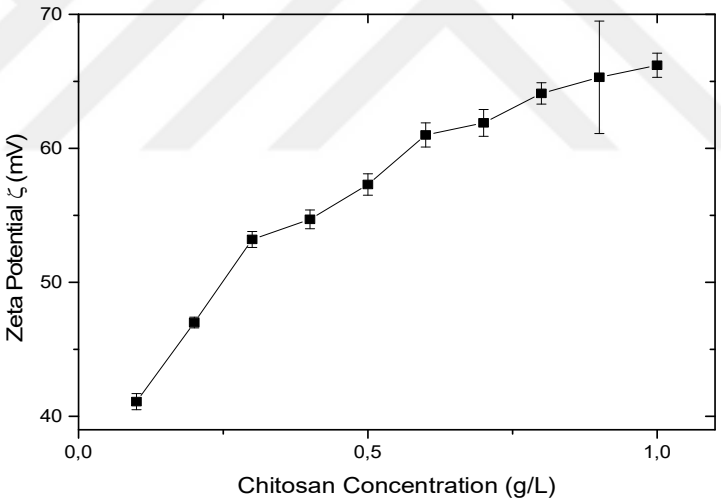

Figure 4.9: Different chitosan concentration response zeta potential values.

The concentrations above 0.1 g/L were resulted in positively charged surfaces. The changes of the surfaces from negative to the positive values were obtained for lower concentrations of 10^{-2} g/L additions. Hence, chitosan concentration was reordered between 10^{-5} and 10^{-2} g/L.

Figure 4.10 shows that low concentration chitosan coated IOPs caused to electrostatic repulsions between chitosan polymers. Increasing concentration of chitosan coated IOPs break the flocs and reduce the interaction of particles. The

surfaces of the IOPs fully covered stable dispersions of the particles obtained with 10^{-2} g/L C-IOPs and 10^{-3} g/L C-IOPs. They will be examined in different pH conditions.

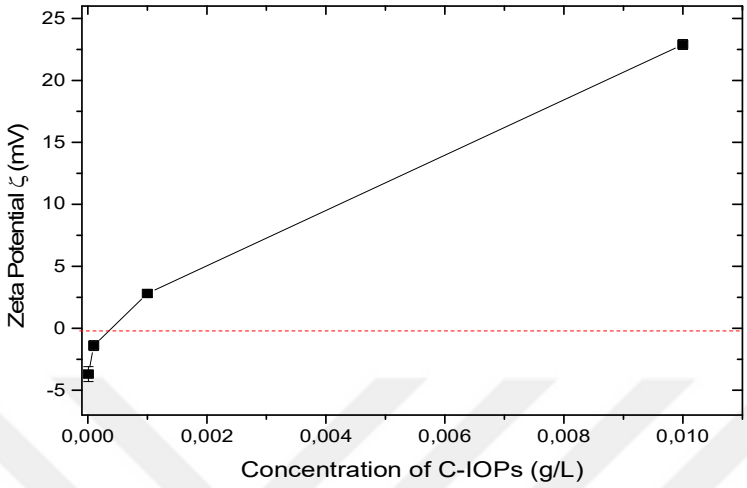

Figure 4.10: Different concentrations of C- IOPs and their zeta potential values.

Table 4.9 shows zeta potential values of chitosan coated IOPs in acidic and basic conditions. The dispersions whose have absolute value of zeta potential values bigger than 25 mV are called stable dispersions.

Table 4.9: Zeta potential (mV) values of different pH levels on chitosan-coated IOPs surfaces.

	pH 3.5	**pH 4**	**pH 7.4**	**pH 10**
10^{-3} g/L C-IOPs	34.5±4.3	1.7±2.4	2.25±0.13	-28±4.4
10^{-2} g/L C-IOPs	41.3±5.9	22.9±0.4	-0.6±4	-23±1.2

4.3.2 Rheological properties of C-IOPs

Chitosan-coated and uncoated IOPs exhibit the same shear thickening flow behavior in Figure 4.11. Shear thickening means that the deforming of the material changes the arrangement of its microstructure and causes to increase the resistance to flow with any increase in shear rate.

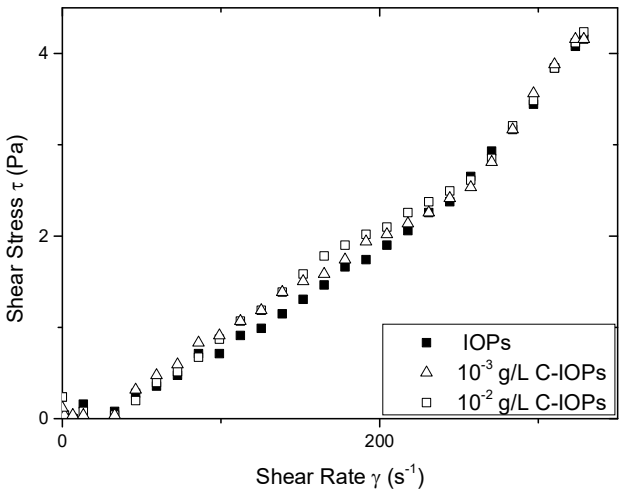

Figure 4.11: Flow curves of chitosan-coated and uncoated IOPs.

Chitosan-coated IOPs covered the whole surfaces and formed flocculations. However, they reduced the interaction of particles with the applied shear rate in some ranges which was seen on the flow curves.

Chitosan-coated IOPs were also investigated in different pH mediums.

Flow curves of 10^{-3} g/L C-IOPs are seen in Figure 4.12 a. All pH conditions except pH 7.4 indicate shear thickening flow type. Addition acid or base did not affect the interaction between particles. However, in pH 7.4, 10^{-3} g/L C-IOPs reduced the interactions of particles and showed nearly Newtonian flow. Flow curves of 10^{-2} g/L C-IOPs show the same shear thickening flow type in all pH conditions in Figure 4.12 b.

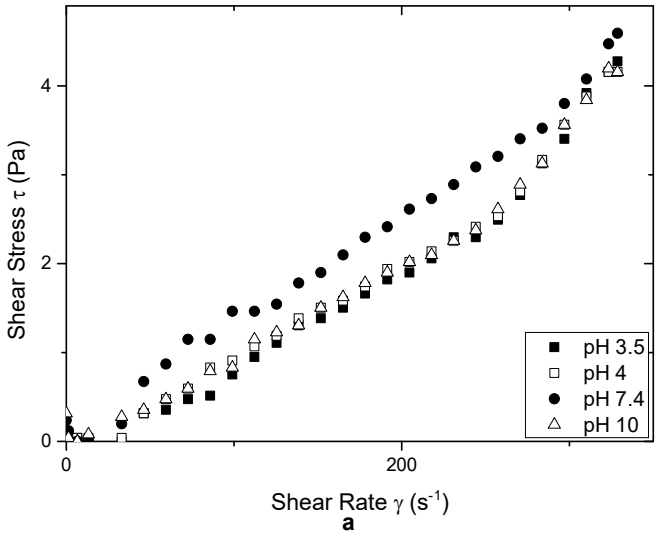

a

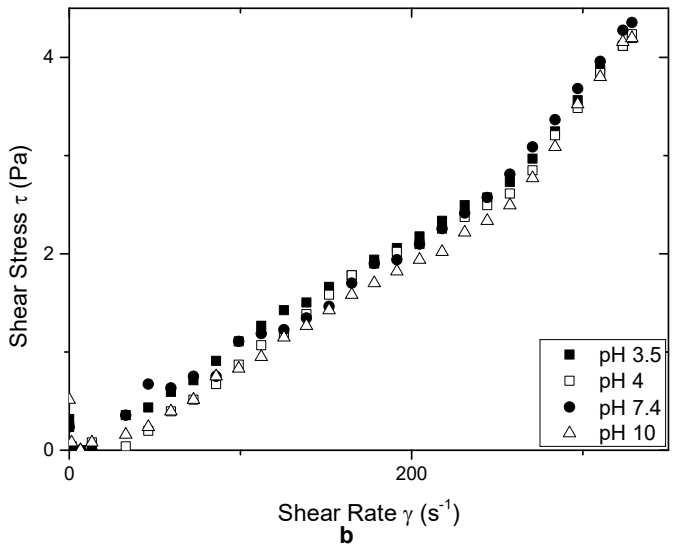

Figure 4.12: Flow curves of (a) 10^{-3} g/L and (b) 10^{-2}g/L C-IOPs in different pH conditions.

Plastic flow slopes shows that, pH 7.4 conditions were caused flocculations of chitosan coated IOPs in Table 4.10.

Table 4.10: Lists of plastic flow slopes of 10^{-3} g/L and 10^{-2} g/L C-IOPs in different pH levels.

pH	10^{-3} g/L C-IOPs Plastic Flow slopes
3.5	2.36 ± 0.09
4	2.34 ± 0.12
7.4	2.13 ± 0.164
10	2.32 ± 0.08
pH	**10^{-2} g/L C-IOPs Plastic Flow slopes**
3.5	2.02 ± 0.05
4	2.17 ± 0.08
7.4	2.07 ± 0.05
10	2.20 ± 0.114

Apparent viscosities at 1.32-328.6 (s^{-1}) shear rates show that 10^{-3} g/L C-IOPs in all pH conditions except pH 3.5 reduce the interaction of particles with the applied shear rate. They have broken the flocs and reduced final viscosity values. The acidic condition caused to increase the interaction of particles and forms flocculations. 10^{-2} g/L C-IOPs reduced the interaction of particles and break the flocculation in all pH conditions as seen in Table 4.11.

Table 4.11: Initial and final shear rate (s^{-1})-Viscosity (Pa.s) values of chitosan-coated IOPs in different pH levels.

10^{-3} g/L C-IOPs	1.32 s^{-1}	328.6 s^{-1}
pH 3.5	0	1.30
pH 4	2.99	1.26
pH 7.4	8.99	1.39
pH 10	2.99	1.26
10^{-2} g/L C-IOPs	**1.32 s^{-1}**	**328.6 s^{-1}**
pH 3.5	2.99	1.27
pH 4	2.99	1.28
pH 7.4	2.99	1.32
pH 10	5.99	1.27

4.3.3 Particle size (DLS) properties of C-IOPs

Chitosan covers the IOPs surfaces and breaks the flocs, so chitosan-coated IOPs reduce the particle sizes compared to IOPs. pH 7.4 caused to agglomeration of chitosan-coated IOPs and increase the particle sizes. Acidic and basic pH conditions affect to particle size. Particle sizes of 10^{-3} g/L C-IOPs increase compared to IOPs, but 10^{-2} g/L C-IOPs decrease in pH 3.5. Basic conditions caused to two different particle size for 10^{-3} g/L C-IOPs. Firstly, they break the flocs and reduce the particle sizes. Besides, they covered flocs surfaces and increased particle sizes. 10^{-2} g/L C-IOPs reduce the particle sizes under basic conditions. They show in Table 4.12.

Table 4.12: Average of particle sizes (d.nm) of chitosan-coated and uncoated IOPs in different pH conditions.

	pH 3.5	pH 4 & 5	pH 7.4	pH 10
IOPs	700	700 (pH 5)	200	700
10^{-3} g/L C-IOPs	900	300	700	300, 1100
10^{-2} g/L C-IOPs	500	500	900	350

4.3.4 FTIR properties of C-IOPs

Figure 4.13 show that addition of the chitosan did not change the spectrum of Fe_3O_4. The polymer addition was too low, so the characteristic peaks of the chitosan did not appear on the spectrum.

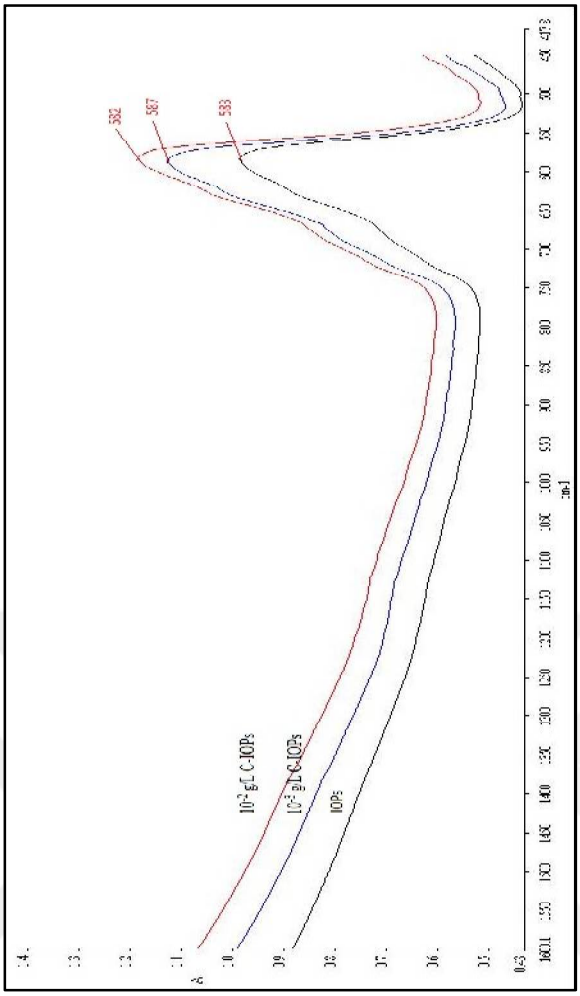

Figure 4.13: FTIR spectrum of chitosan-coated and uncoated IOPs.

4.4 Quartz Crystal Microbalance with Dissipation Results

In the QCM-D experiments, liposomes were added to clean gold surface. After the lipid layerformation, PBS was passed throughflow chamber to removeunbound liposomes on gold surface. The Q-Tools data evaluation software was used to estimate the mass adsorbed in different experiments. Presented calculated changes of frequency (Δf) and dissipation (ΔD) were based on three experiments. All experiments were done in accordance with the physiological pH. First experiments were done to optimize the measurement conditions such as suitable dilutions for coated and uncoated IOPs and constant flow rate.

Three different charged liposomes were prepared and observed in QCM-D by frequency and disipation shift. Zeta potential of PC, PS and DOTAP liposomes was measured as -4.52, -19.6 and 25 mV, respectively. They have around 100-130 nm particle size. Differences of Δf and ΔD were probably arised from different zeta

potential values They show in Figure 4.14. ΔD/Δf states the acoustic ratio representing the energy loss per unit of attached mass and provides both qualitative and quantitative information on the instrinsic properties and morphology of the sensed interface. Especially, ΔD/Δf ratio would depend on the deposited mass, its viscoelastic properties and the shape and structure of the liposomes. In QCM-D, gold-coated quartz sensor surface is hydrophilic. This surface helps to attach hydrophilic head group of liposomes. Therefore, differences of acoustic ratio of liposomes as seen in Figure 4.14 arised from van der Waals and repulsive forces between liposomes and gold coated quartz surface. Gold surface and 25% DOTAP:PC interacted strongly with van der Waals forces, while surface and 25% PS:PC liposome interact loosly, so acoustic ratio is lower than others.

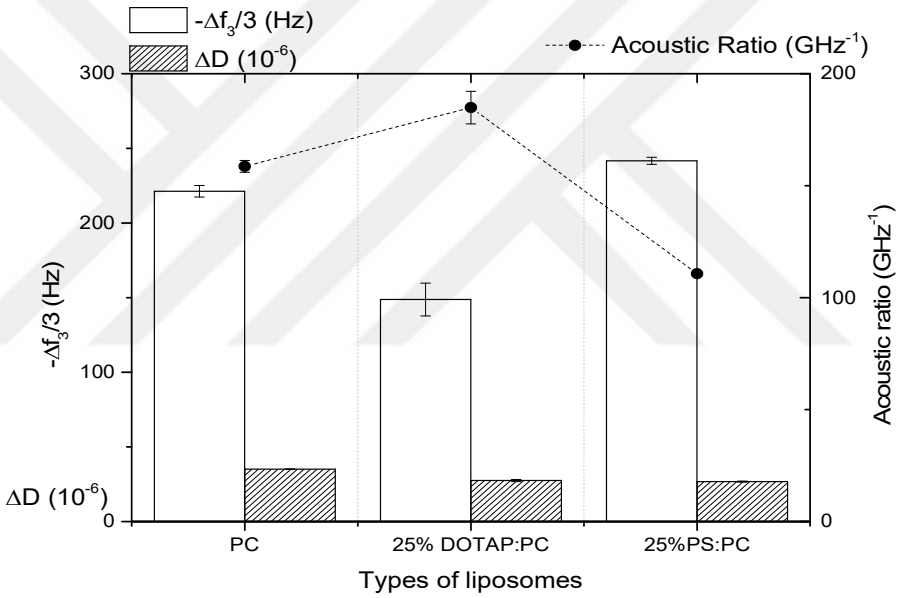

Figure 4.14: Changes of frequency and dissipation on different types of liposomes.

After liposome layer was introduced to the surface, this cell membrane model was treated with chitosan coated and uncoated IOPs at different dilutions. According to Figure 4.15, two fold dilution affected both frequency and dissipation higher than other dilutions for both uncoated and chitosan coated IOPs. This value is much higher than expected individual particle binding to the surface so it is probably the result of accumulation of high number of particles or aggregates on the surface. Optimum dilution was chosen as three fold because it seems to reduce the excessive aggregate formation.

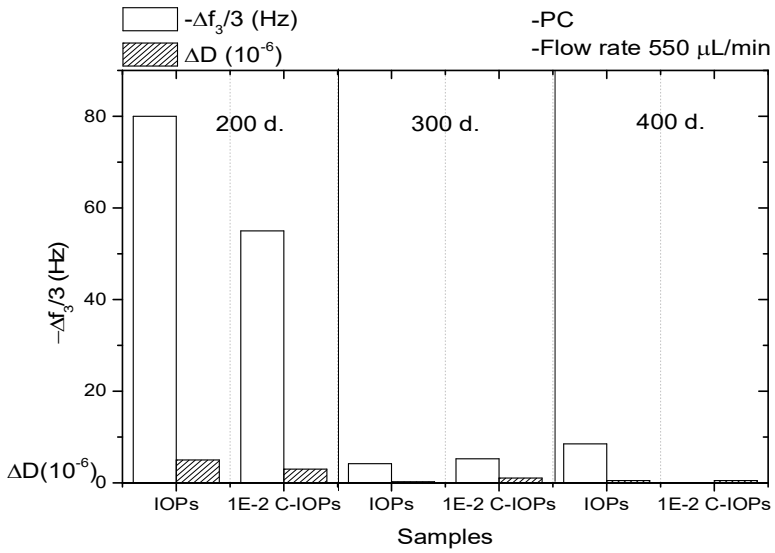

Figure 4.15: Effects of dilutions to evaluate interaction of C-IOPs and uncoated IOPs with PC liposome layer at constant flow rate (d.: dilution).

After the optimization, interaction of uncoated, PVA and chitosan coated IOPs on three different liposome layers, formed by the addition of different lipids, was investigated by QCM-D technique. In these experiments, liposomes were added to clean gold surface. After the liposome layer formation, PBS was passed through flow chamber to remove unbound liposomes on gold surface. After that, coated and uncoated IOPs were introduced to reaction chamber. When IOPs and liposome interactions were stabilized, unbound/loosely bound IOPs was washed with PBS. The Q-Tools data evaluation software (Biolin Scientific, Sweden) was used to estimate the mass adsorbed in different experiments. Presented calculated changes of frequency and dissipation were based on three experiments.

4.4.1 Results on phosphatidylcholine (PC) liposome layer

Phosphatidylcholine (PC) is a zwitterionic or neutral lipid as seen in Figure 4.16. In this experiment, prepared PC liposomes had -4.52 zeta potential values at physiological pH 7.4.

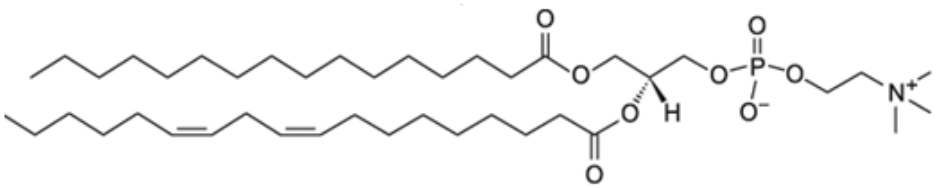

Figure 4.16: The chemical structure of phosphatidylcholine (PC) (Url-4).

According to changes of frequencies, C-IOP introduction affected PC liposome layer higher than PVA-coated and uncoated IOPs as seen in Figure 4.17. Sizes of chitosan-coated IOPs are higher than uncoated, PVA-coated IOPs, and this could be the reason behind this. Acoustic ratio of PVA-coated samples is significantly high. High dissipation values for these particles showed that some particles interacted/incorporated to the liposome layer as C-IOPs but led to more viscoelastic layer may be because there smaller.

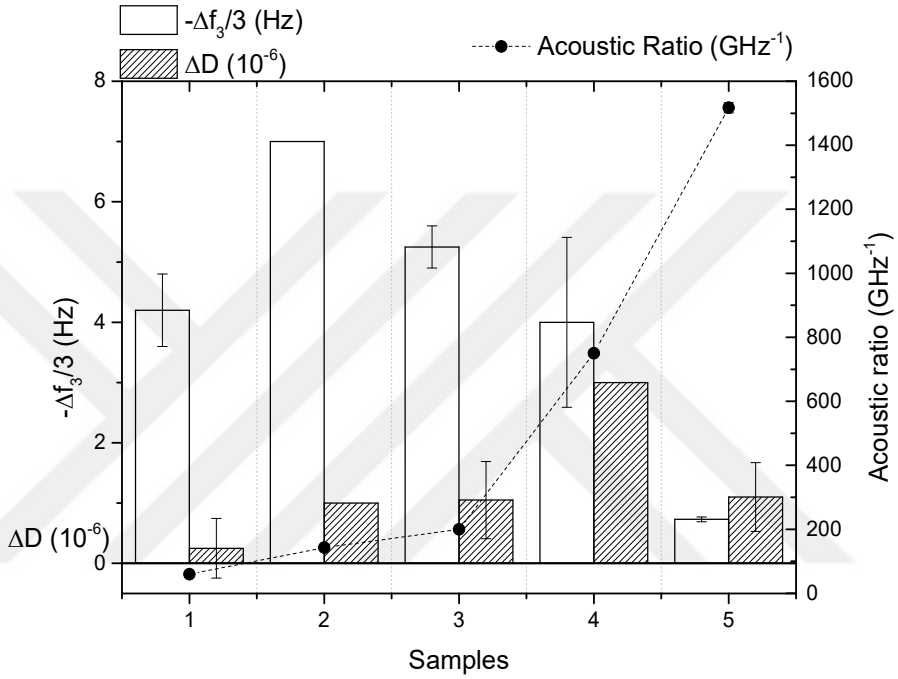

Figure 4.17:Changes of Δf and ΔD of coated and uncoated IOPs on PC liposome layer.

(1- IOPs, **2-**10^{-3} g/L-C-IOPs, **3-** 10^{-2} g/L- C-IOPs, **4-**0.5 g/L PVA-IOPs, and **5-** 1.0 g/L PVA-IOPs)

Figure 4.18 and Figure 4.19 show the time dependent frequency and dissipation changes recorded continuously until steady state condition for coated and uncoated IOPs. Chitosan-coated and uncoated IOPs remove the liposome layer on the gold surface (increase in frequency), however, PVA-coated IOPs were attached to the layer. Changes of dissipation give information about elastiscity or rigidity. Figure 4.19 shows that uncoated IOPs and 10^{-2} g/L C-IOPs do not change dissipation Consequently, according to frequency and dissipation data of these samples, it seems that they form a rigid layer on surface. The amount of PVA coating also affected dissipation. When the amount of PVA increased, dissipation was also increased.

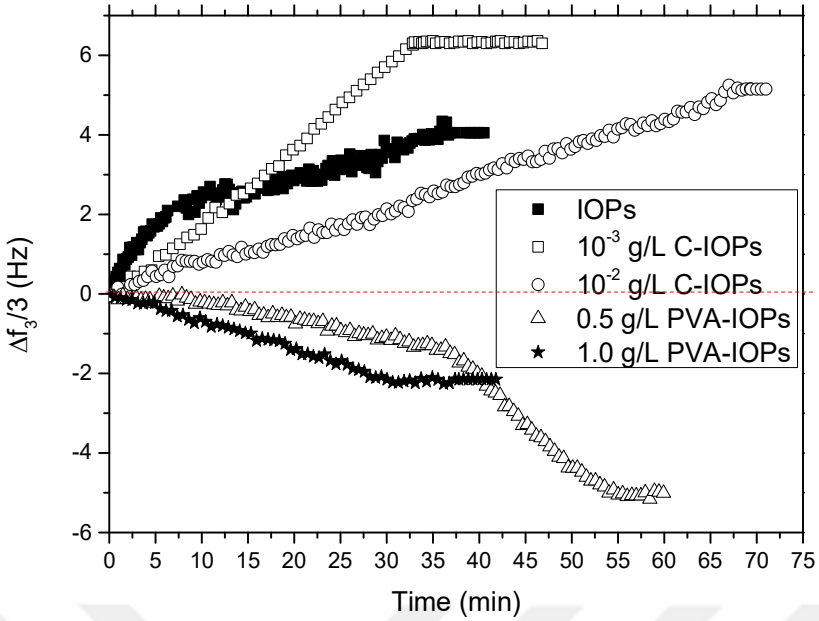

Figure 4.18: Changes of frequency with time of polymer-coated and uncoated IOPs.

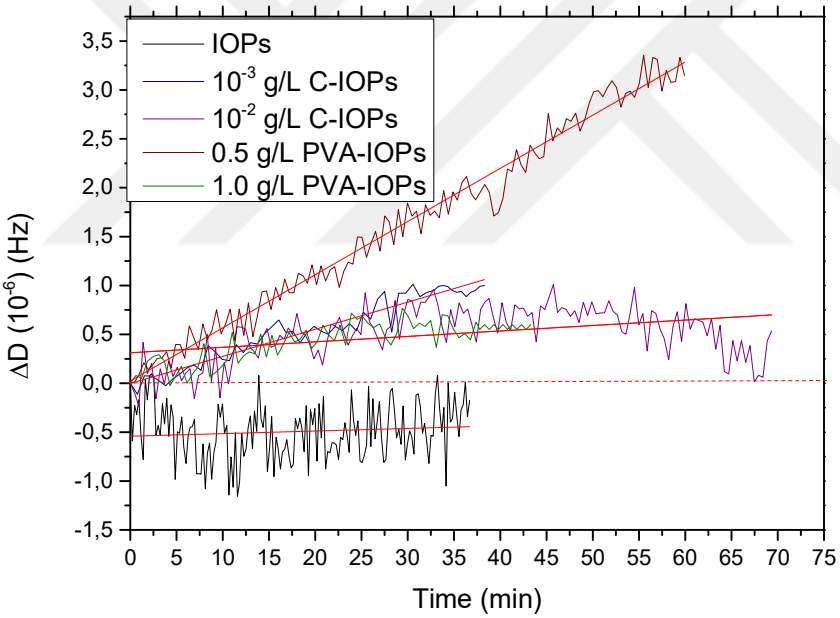

Figure 4.19: Changes of dissipation with time of polymer-coated and uncoated IOPs.

4.4.2 Results on 25% phosphatidylserine (PS): phosphatidylcholine (PC) liposome layer

Phosphatidylserine (PS) is an anionic and acidic phophalipid with neutral head group and negatively charged phosphate group as seen in Figure 4.20. Therefore, it carries one negative charge at pH 7 (Meer et al, 2008; Leventis & Grinstein, 2010). In this experiment, prepared PC liposome layer contain 25% PS and its zeta potential value was -19.6.

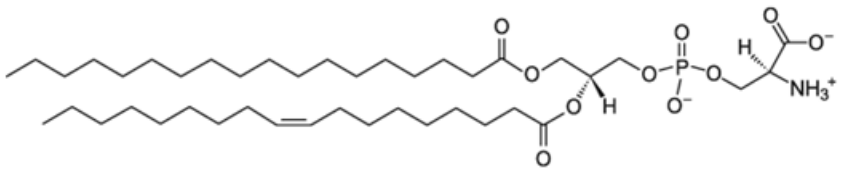

Figure 4.20: The chemical structure of phosphatidylserine (PS) (Url-5).

According to changes of frequencies of samples, PVA-coated IOPs affected 25% PS:PC liposome layer higher than uncoated and chitosan-coated IOPs. They show in Figure 4.21. Zeta potential value of IOPs is -17 mV in pH 7.4. IOPs and 25% PS:PC liposome probably could not interact strongly, consequently, this caused low frequency and dissipation change than coated IOPs. Dissipation changes of polymer coated samples may arise from particle sizes.

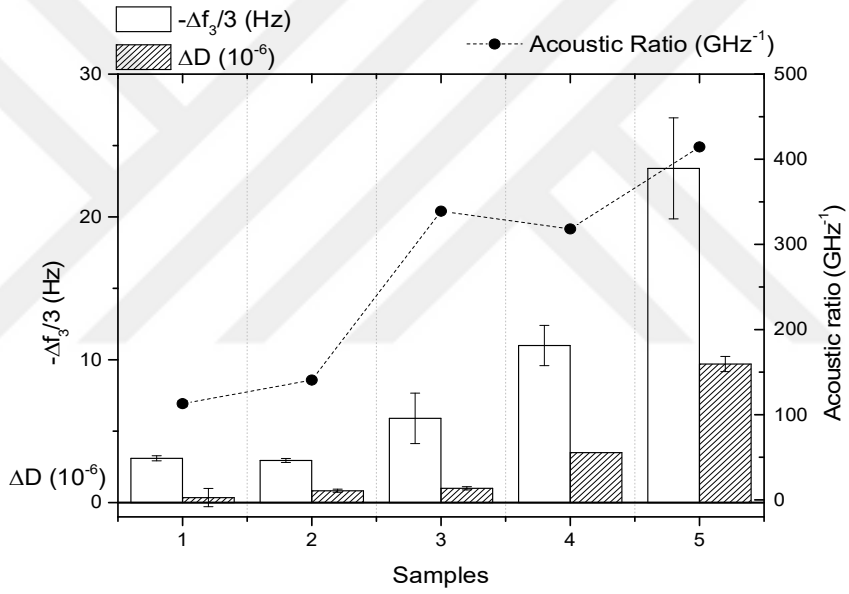

Figure 4.21: Changes of Δf and ΔD of coated and uncoated IOPs on 25% PS:PC liposome layer.

(1- IOPs, **2-** 10^{-3} g/L C-IOPs, **3-** 10^{-2} g/L C-IOPs, **4-** 0.5 g/L PVA-IOPs and **5-** 1.0 g/L PVA-IOPs)

Figure 4.22 and Figure 4.23 show changes of frequency and dissipation in versus time for coated and uncoated IOPs. High PVA coating (1.0 g/L) and low chitosan-coated (10^{-3} g/L) IOPs removes 25% PS:PC layer but the effect of PVA ones are higher. C-IOP one also had no significant change in dissipation so it seems that not much interaction occurs. Uncoated IOPs and other samples were attached to the liposome layer. Significant dissipation changes can only be seen in 0.5 g/L PVA-IOPs and 1.0 g/L PVA-IOPs samples but the later one reduced it.

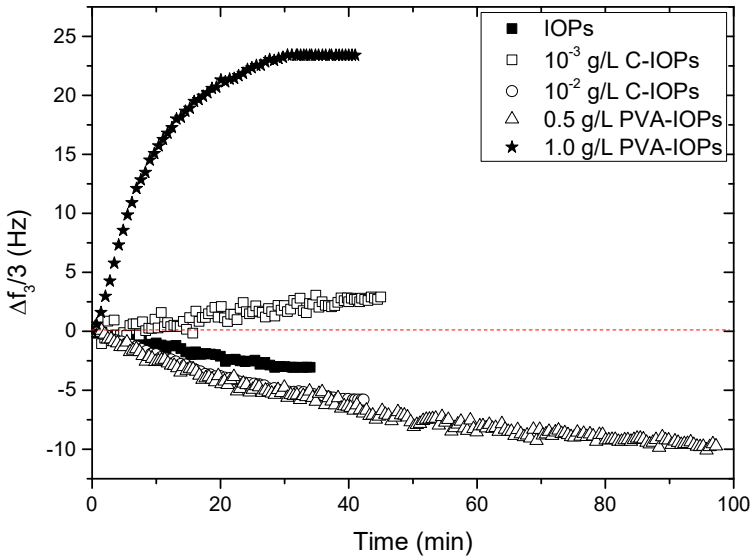

Figure 4.22: Changes of frequency with time of polymer coated and uncoated IOPs on 25% PS:PC liposome layer.

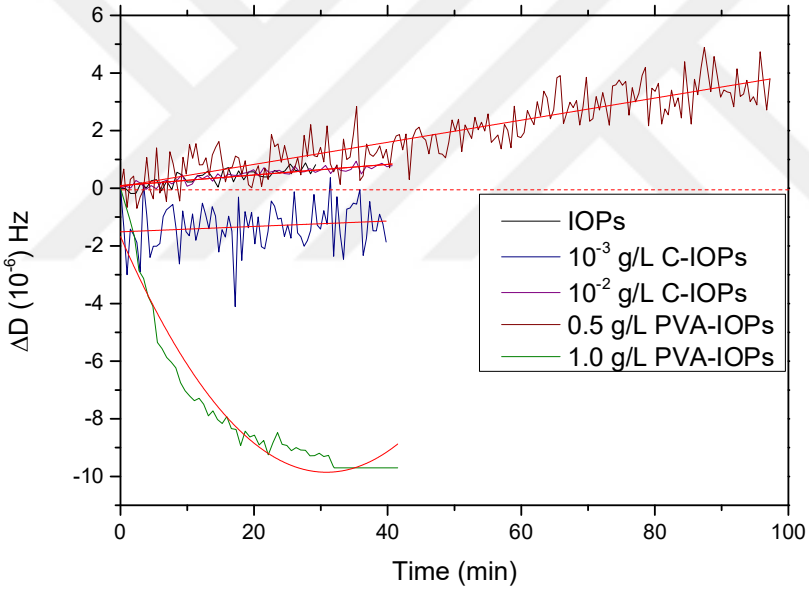

Figure 4.23: Changes of dissipation with time of polymer coated and uncoated IOPs on 25% PS:PC liposome layer.

4.4.3 Results on 25% 1,2-dioleoyl-3-trimethylammonium-propane (DOTAP): phosphatidylcholine (PC) liposome layer

1,2-dioleoyl-3-trimethylammonium-propane (DOTAP) is a synthetic and cationic phospholipid. It have one positive charge on ammonium group. Figure 4.24 showed chemical structure it. In this experiment, zeta potential of prepared 25% DOTAP:PC liposomes was measured as 25 mV.

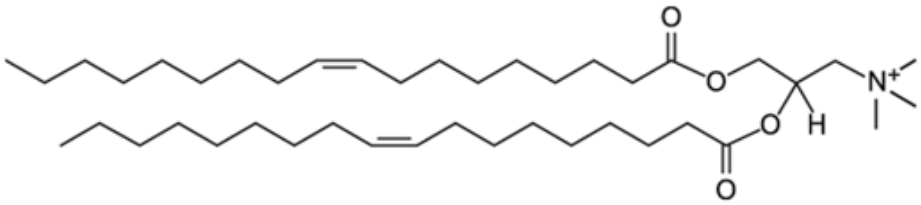

Figure 4.24: The chemical structure of 1,2-dioleoyl-3-trimethylammonium-propane (DOTAP) (Url-6).

Figure 4.25 shows that, uncoated IOPs' interaction with liposome layer is the highest probably due to electrostatic interactions. Chitosan coated IOPs gave higher frequency than PVA coated IOPs for 25% DOTAP:PC liposome layer which could be resulted from their size. Acoustic ratio values did not show any conclusive trend so it should be studied further to comment on the nature of these interactions.

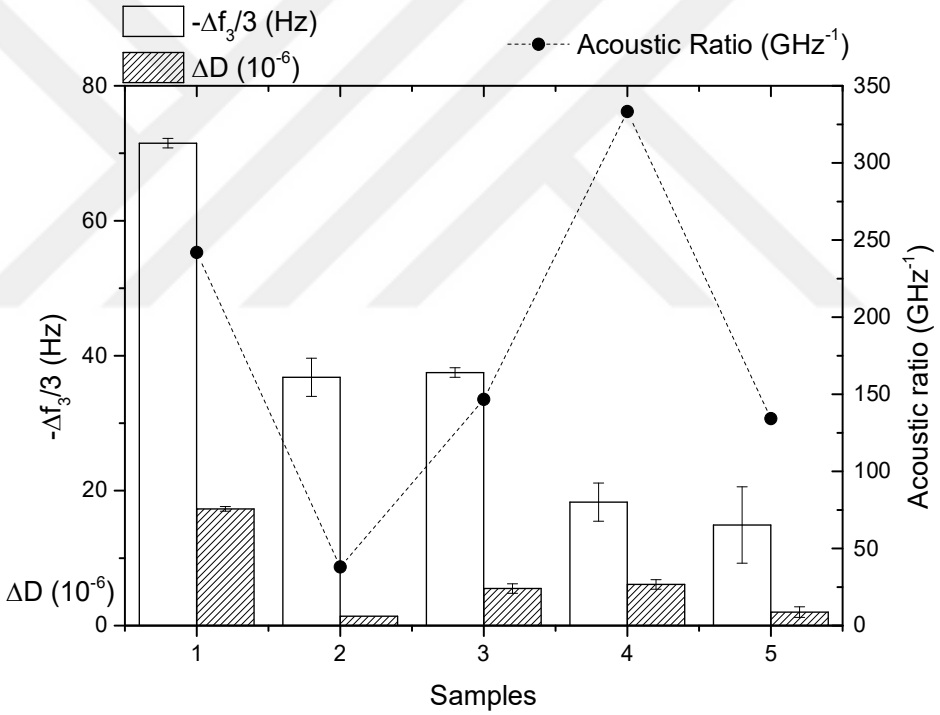

Figure 4.25: Changes of Δf and ΔD of coated and uncoated IOPs on 25% DOTAP:PC liposome layer.

(1- IOPs, **2-**10^{-3} g/L C-IOPs, **3-** 10^{-2} g/L C-IOPs, **4-**0.5 g/L PVA-IOPs, and **5-** 1.0 g/L PVA-IOPs)

Figure 4.26 shows time dependent frequencies changes of polymer coated and uncoated IOPs. All of the samples seemed type interact and remove the liposome layer. According to changes in frequency, uncoated IOPs affect to liposome layer higher than polymer coated IOPs with electrostatically. When the amount of chitosan

in coating was increased, the attachment of particles on liposome layer increased further.

Figure 4.27 showed that uncoated IOPs were not only attached 25% DOTAP:PC to liposome layer but also caused an increase in the viscoelastic behavior of the liposome layer.

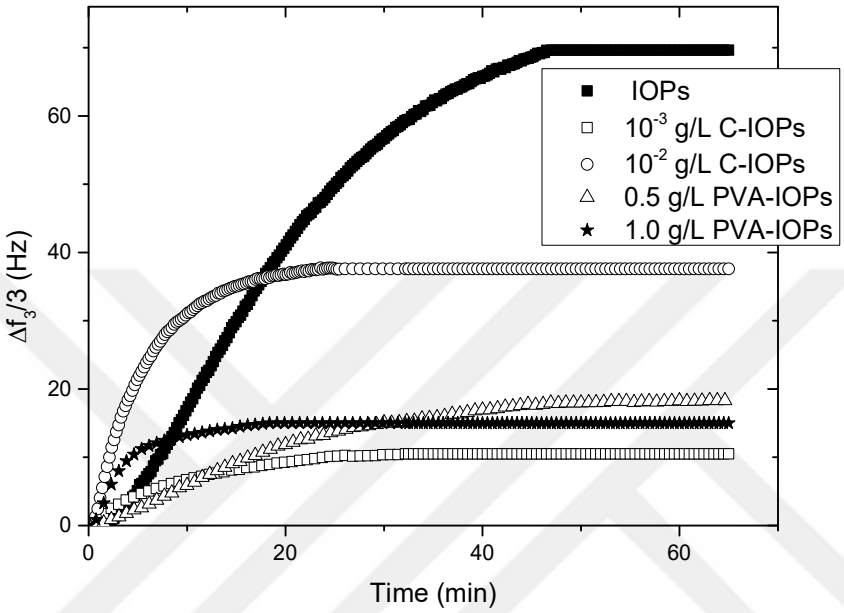

Figure 4.16: Changes of frequency with time of polymer coated and uncoated IOPs on 25% DOTAP:PC liposome layer.

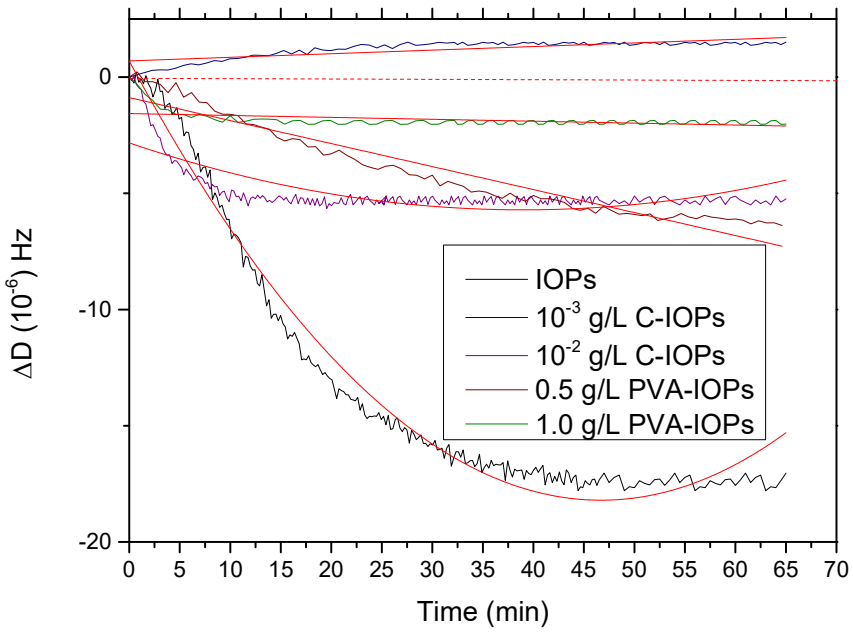

Figure 4.27: Changes of dissipation with time of polymer coated and uncoated IOPs on 25% DOTAP:PC liposome layer.

CONCLUSIONS AND RECOMMENDATIONS

In this study, the goal was to synthesize polymer coated IOPs to reduce their toxicity and to investigate their interaction with cell membranes using liposomes, a model membrane system. Prepared polymer-coated IOPs were characterized at different pH conditions. In addition, the interaction of coated and uncoated IOPs were investigated with positive, neutral and negatively charged liposome layers by QCM-D technique.

PVA and chitosan were chosen to coat the IOPs' surfaces because of their biodegradable and biocompatible properties. PVA and chitosan are ionizable polymers and therefore they are positively charged in acidic media and negatively charged in basic media. Their physical and chemical properties consequently change in different pH conditions. Polymer-coated and uncoated IOPs were also examined in physiological pH conditions to observe their interaction with cell membrane by using QCM-D. PVA and chitosan are neutral in PBS (pH 7.4).

Size, charge, shape and interface properties play critical role for the formation of stable suspension in colloidal systems. Particle-particle interactions affect flow behavior, size and viscosity. IOPs tend to agglomeration or flocculation. In all pH conditions, IOPs dispersion is unstable and in the aggregating regime. 0.5 g/L and 1.0 g/L PVA-IOPs examined in different pH conditions. Obtained measurements results show that 1.0 g/L PVA cover the whole surfaces of the IOPs compared to 0.5 g/L PVA. Besides, the IOPs were covered with chitosan polymer at different concentrations. The results show that 10^{-2} g/L C-IOPs cover the whole surfaces of IOPs and optimum pH is 4. PVA caused to increase the interactions of particles and form flocculation, however, chitosan prevent the forming of flocculation and reduce particle interactions. These results also seemed to affect the interaction of IOPs with liposome layer in QCM-D. Differently charged liposomes were prepared to see the effect of electrostatic interactions on nanoparticle toxicity. Electrostatic interactions largely affects attachment or disruption of a cell membrane. Polymer coated IOPs in PBS have neutral zeta potential, but IOPs have negative charge. It could be seen that

interaction of all particles with PC liposomes is the lowest with -Δf values in between 1-7 Hz. When PS, a negatively charged lipid was added, interactions become more significant (-Δf = 4-22 Hz) and PVA coated IOPs seemed to have higher interaction with this layer. This could also be the effect of particle size on the surface. When PS was replaced by DOTAP, the situation was reversed and lowest interaction was recorded for PVA coated IOPs. It should be noted that highest frequency shifts (15-70 Hz) were observed on 25% DOTAP:PC layer. Although, electrical interactions seem to be important, particle size also affect the extent of interaction and therefore more thorough studies should be done to have a better understanding on this complex phenomena.

In the future studies, magnetorheometers can be used for studying the changes in flow properties under magnetic field for targeted drug delivery and thermogravimetric analysis can be done to measure of the effectiveness of particles for hyperthermia treatment. Moreover, chemotherapeutic drugs can be loaded into these particles and cell culture studies can be done to compare the results with QCM-D data.

REFERENCES

Atala, A., Irvine, D. J., Moses, M., & Shaunak, S. (2010). Wound healing versus regeneration: Role of the tissue environment in regenerative medicine. *MRS Bulletin / Materials Research Society*, *35*(8), 10.1557/mrs2010.528. http://doi.org/10.1557/mrs2010.528

Baker, M. I., Walsh, S. P., Schwartz, Z. & Boyan, B. D. (2012), A review of polyvinyl alcohol and its uses in cartilage and orthopedic applications . *J. Biomed. Mater. Res.*, 100B: 1451-1457. doi:10.1002/jbm.b.32694

Bashar, M.M.. & Khan, M.A. (2013), An overview on surface modification of cotton fiber apparel use. *J Polym Environ*, 21: 181. https://doi.org/10.1007/s10924-012-0476-8

Bekaroglu, M. G., Isci, Y. & Isci, S. (2017). Colloidal properties and in vitro evaluation of Hydroxy ethyl cellulose coated iron oxide particles for targeted drug delivery. *Materials Science and Engineering: C.* 78, 847-853. https://doi.org/10.1016/j.msec.2017.04.030.

Brandenburg, U., & Lagaly, G. (1988). Rheological properties of sodium montmorillonite dispersions. *Applied Clay Science, 3*(3), 263-279. doi:https://doi.org/10.1016/0169-1317(88)90033-6

Bradshaw L.(2000) Understanding piezoelectric quartz crystals. *RF time and frequency* 8:50–58.

Cho, N. J, Kanazawa, K. K., Glenn, J. S., & Frank, C. W. (2007). Employing Two Different Quartz Crystal Microbalance Models To Study Changes in Viscoelastic Behavior upon Transformation of Lipid Vesicles to a Bilayer on a Gold Surface, *Anal. Chem., 79*, pp. 7027-7035.

Chou, C. K., Chen, S. M., Li, Y. C., Huang, T. C., & Lee, J. A. (2015). Low-molecular-weight chitosan scavenges methylglyoxal and N^{ε}-(carboxyethyl) lysine, the major factors contributing to the pathogenesis of nephropathy. *SpringerPlus*, *4*, 312. http://doi.org/10.1186/s40064-015-1106-4

Coey, J. M. D. (2009). *Magnetism and Magnetic Materials*. Cambridge University Press.

Everett, D. H.: *Basic Principles of Colloid Science. London, Royal Society of Chemistry, 1988, 243 S., 106 Abb., 4 Tab., 120 Lit., broschiert, £ 9,95, ISBN 0–85186–443–0*

DeMerlis, C. C. & Schoneker, D. R. (2003). Review of the oral toxicity of polyvinyl alcohol (PVA). *Food and Chemical Toxicology,* 41 (3), 319-326. https://doi.org/10.1016/S0278-6915(02)00258-2.

Derjaguin, B. & Landau, L. (1993). Theory of the stability of strongly charged lyophobic sols and of the adhesion of strongly charged particles in solutions of electrolytes. *Progress in Surface Science,* 43 (1-4), 30-59. https://doi.org/10.1016/0079-6816(93)90013-L.

Dickinson, E. (1989), Basic principles of colloid science: By D. H. Everett, Royal Society of Chemistry, London, 1988. Paperback, pp. xv + 243, price £9.95, $ 19.50. ISBN 0-85186-443-0. J. Chem. Technol. Biotechnol., 45: 328-329. doi:10.1002/jctb.280450412

Dixon, M. C. (2008). Quartz Crystal Microbalance with Dissipation Monitoring: Enabling Real-Time Characterization of Biological Materials and Their Interactions, *Journal of Biomolecular Techniques,* 19, pp. 151-158.

Eliassaf, J. (1972), Detection of small quantities of poly(vinyl alcohol) in poly(vinyl chloride) resins. *J. Polym. Sci. B Polym. Lett.,* 10: 697-698. doi:10.1002/pol.1972.110100907

Elieh-Ali-Komi, D. & Hamblin, M. R. (2016). Chitin and chitosan: production and application of versatile biomedical nanomaterials. *International Journal of Advanced Research*, *4*(3), 411–427

Errington, N., Harding, S. E., Varum, K. M. & Illum, L. (1993). Hydrodynamic characterization of chitosans varying in degree of acetylation. *International Journal of Biological Macromolecules*, 15 (2), 113-117. https://doi.org/10.1016/0141-8130(93)90008-A.

Finch, R. M. (1984), Principles of colloid and surface chemistry, by Paul C. Hiemenz, Marcel Dekker, New York, 1977, 516 pp. No Price given. *J. Polym. Sci. B Polym. Lett. Ed.,* 22: 508-509. doi:10.1002/pol.1984.130220910.

Hackley, V. A. & Ferraris, C. F. (2001). Guide to Rheological Nomenclature: Measurement in Ceramic Particulate Systems. Special Publication (NIST SP) – 946

Henry, S. A., Kohlwein, S. D. & Carman, G. M. (2012). Metabolism and regulation of glycerolipids in the yeast Saccharomyces cerevisiae. 190 (2): 317-49. Doi: 10.1534/genetics.111.130286

Hiemenz, P. C. & Rajagopalan, R. (1997). *Principles of Colloid and Surface Chemistry*, Marcel Dekker, Newyork.

No, H. K. & Meyers, S. P. (1995) Preparation and characterization of chitin and chitosan—A Review, *Journal of Aquatic Food Product Technology*, 4:2, 27-52, DOI: 10.1300/J030v04n02_03

Hunter, R. J. (1981). Chapter 2 - Charge and potential distribution at interfaces. In R. J. Hunter (Ed.), *Zeta Potential in Colloid Science* (pp. 11-58): Academic Press.

Islam, S., Bhuiyan, M.A.R. & Islam, M.N. (2017). Chitin and chitosan: structure, properties and applications in biomedical engineering. *J.Polymers and Environment*, 25: 854. https://doi.org/10.1007/s10924-016-0865-5.

Isci, S., Isci, Y. & Bekaroglu, M. G. (2017). Particle interactions of polyvinylpyrrolidone-coated iron oxide particles as magnetic drug delivery agents. Appl. Phys. A, 123: 534. https://doi.org/10.1007/s00339-017-1146-4.

Jakubovics, J. P. (1994). *Magnetism and magnetic materials,* Institute of Materials.

Jiles, D. (1998*). Introduction to Magnetism and Magnetic Materials*, London, CRC Press.

Jones, J. I. (1973), Polyvinyl alcohol. Properties and applications. Edited by C. A. Finch. John Wiley, Chichester. 1973. Pp. xviii + 622. Price: £14.00. Brit. Poly. J., 5: 493-494. doi:10.1002/pi.4980050608

Jordan, A., Scholz, R., Wust, P., Fähling, H. & Felix, R. (1999). Magnetic fluid hyperthermia (MFH): Cancer treatment with AC magnetic field induced excitation of biocompatible superparamagnetic nanoparticles. *Journal of Magnetism and Magnetic Materials,* 201 (1-3), 413-419. https://doi.org/10.1016/S0304-8853(99)00088-8.

Israelachvili, J. N. (2011). Fundamental Constants. In J. N. Israelachvili (Ed.), *Intermolecular and Surface Forces (Third Edition)* (pp. 1). Boston: Academic Press.

Jiang, J., Oberdorster, G., Elder, A., Gelein, R., Mercer, P., & Biswas, P. (2008). Does Nanoparticle activity depend upon size and crystal phase? *Nanotoxicology, 2*(1), 33-42. doi:10.1080/17435390701882478

Kanazawa, K., & Nam-Joon, C. (2009). Quartz Crystal Microbalance as a Sensor to Characterize Macromolecular Assembly Dynamics, *Journal of Sensors.*

Krishnan, K. M. (2010). "Biomedical Nanomagnetics: A Spin Through Possibilities in Imaging, Diagnostics, and Therapy. *IEEE Transactionson Magnetics*, 46(7), 2523–2558. doi:10.1109/TMAG.2010.2046907

Kulkarni, P., Sureshkumar, R., & Biswas, P. (2003). Multiscale simulation of irreversible deposition in presence of double layer interactions. *J Colloid Interface Sci, 260*(1), 36-48.

Laurent, S., Forge, D., Port, M., Roch, A., Robic, C., Elst, V. L. & Muller, R. N. (2010). Magnetic Iron Oxide Nanoparticles: Synthesis, Stabilization, Vectorization, Physicochemical Characterizations, and Biological Applications. *Chemical Reviews*. *110* (4), 2574-2574, DOI: 10.1021/cr900197g

Lee, J. H., Jang, J. T., Choi, J.S., Moon, S.H., Noh, S. H., Kim, J. W., Kim, J. G., Kim, I. S., Park, K. I. & Cheon, J. (2011). Exchange-coupled magnetic nanoparticles for efficient heat induction. *Nat Nanotechnol.* 26;6(7):418-22. doi: 10.1038/nnano.2011.95.

Leslie-Pelecky, D. L. & Rieke, R. D. (1996). Magnetic Properties of Nanostructured Materials. *Chemistry of Materials.* 8(8): 1770-1783.

Leventis, P. A. & Grinstein, S. (2010). The distribution and function of phosphatidylserine in cellular membranes. *Annu. Rev.Biophys.* 39:407-27. doi: 10.1146/annurev.biophys.093008.131234.

Luckham, P. F. & Rossi, Sylvia. (1999). The colloidal and rheological properties of bentonite suspensions. *Advances in Colloid and Interface Science*. 82 (1-3), 43-92. https://doi.org/10.1016/S0001-8686(99)00005-6.

Lucklum, R., Behling, C., Cernosek, R.W. & Martin, J.S. (1997). Determination of complex shear modulus with thickness shear mode resonators. *Journal of Physics: D Applied Physics*. 10.1088/0022-3727/30/3/006

Mahmoudi, M., Sant, S., Wang, B., Laurent, S. & Sen, T. (2011). Superparamagnetic iron oxide nanoparticles (SPIONs): Development, surface modification and applications in chemotherapy. Advanced Drug Delivery Reviews, 63, 24-46.

Mahmoudi, M., Simchi, A., Imani, M., Shokrgozar, M.A., Milani, A.S., Häfeli, U.O. & Stroeve P. (2010). A new approach for the in vitro identification of the cytotoxicity of superparamagnetic iron oxide nanoparticles. *Colloids Surf B Biointerfaces.* 75(1):300-9. doi:10.1016/j.colsurfb.2009.08.044.

Matos, C., Moutinho, C. & Lobão, P. (2012). Liposomes as a model for the biological membrane: studies on daunorubicin bilayer interaction. *J. Membrane Biol.* 245: 69. https://doi.org/10.1007/s00232-011-9414-2.

Matthew, A., & Victoria, T. (2007). A Survey of the 2001 to 2005 quartz crystal microbalance biosensor literature: applications of acoustic physics to analysis of biomolecular interactions, *Journal of Molecular Recognation, 20*, no. 3, pp. 154-184.

Matthews, B. A. & Rhodes, C. T. (1970). Use of the Derjaguin, Landau, Verwey, and Overbeek Theory to Interpret Pharmaceutical Suspension stability. *Journal of Pharmaceutical Sciences.* 59 (4), 521-525. https://doi.org/10.1002/jps.2600590417.

McBride, M. , Sauve, S. & Hendershot, W. (1997), Solubility control of Cu, Zn, Cd and Pb in contaminated soils. *European Journal of Soil Science,* 48: 337-346. doi:10.1111/j.1365-2389.1997.tb00554.x

Meer, G., Voelker, D. R. & Feigenson, G. W. (2008). Membrane lipids: where they are and how they behave. *Nat. Rev. Mol. Cell Biol.* 9(2):112-24. doi: 10.1038/nrm2330.

Montes Ruiz-Cabello, F. J., Maroni, P., & Borkovec, M. (2013). Direct measurements of forces between different charged colloidal particles and their prediction by the theory of Derjaguin, Landau, Verwey, and Overbeek (DLVO). *J Chem Phys, 138*(23), 234705. doi:10.1063/1.4810901

Nicolson, G. L. (2014). The fluid—mosaic model of membrane structure: still relevant to understanding the structure, function and dynamics of biological membranes after more than 40years. *Biochimica et Biophysica Acta (BBA) – Biomembranes.*1838 (6), 1451-1466. https://doi.org/10.1016/j.bbamem.2013.10.019.

Nosrati, H., Adinehvand, R., Manjili, H. K., Rostamizadeh, K., & Danafar, H. (2018) Synthesis, characterization, and kinetic release study of

methotrexate loaded mPEG–PCL polymersomes for inhibition of MCF-7 breast cancer cell line, *Pharmaceutical Development and Technology*, doi: 10.1080/10837450.2018.1425433

Oghabian, M. A., Gharehaghaji, N., Amirmohseni, S., Khoei, S. & Guiti, M. (2010). Detection sensitivity of lymph nodes of various sizes using USPIO nanoparticles in magnetic resonance imaging. *Nanomedicine: Nanotechnology, Biology and Medicine.* 6 (3), 496-499. https://doi.org/10.1016/j.nano.2009.11.005.

Ohshima, H. (2014). Chapter 1 - Interaction of colloidal particles. In H. Ohshima & K. Makino (Eds.), *Colloid and Interface Science in Pharmaceutical Research and Development* (pp. 1-28). Amsterdam: Elsevier.

Peetla, C., Stine, A. & Labhasetwar, V. (2009). Biophysical interactions with model lipid membranes: applications in drug discovery and drug delivery. *Molecular Pharmaceutics*. *6* (5), 1264-1276, DOI: 10.1021/mp9000662

Qiao, X., Zhang, X., Tian, Y. & Meng, Y. (2016). Progresses on the theory and application of quartz crystal microbalance. *Applied Physics Reviews.* 3, 031106 https://doi.org/10.1063/1.4963312

Rodahl M, Höök F, Krozer A, Brzezinski P, Kasemo B. (1995). Quartz crystal microbalance set up for frequency and Q-factor measurements in gaseous and liquids environments. *Rev Sci Inst* 66:3924–3930.

Schramm, L. L. (1996). Suspensions: Basic principles. In *Suspensions: Fundamentals and Applications in the Petroleum Industry* (Vol. 251, pp. 3-44): American Chemical Society.

Shaw, D. J. (1992). 8 - Colloid stability. In D. J. Shaw (Ed.), *Introduction to Colloid and Surface Chemistry (Fourth Edition)* (pp. 210-243). Oxford: Butterworth-Heinemann.

Ayyappan, S., Philip, J & Raj, B. (2009). "Solvent polarity effect on physical properties of CoFe2O3 nanoparticles". *J. Phys. Chem. C*. 113: 590–596. doi:10.1021/jp8083875

Singh, N., Manshian, B., Jenkins, G.J.S:, Griffiths, S.M., Williams, P.M., Maffeis, T.G.G., Wright, C. J. & Doak, S.H. (2009). NanoGenotoxicology: The DNA damaging potential of engineered nanomaterials. *Biomaterials.* 30 (23-24), 3891-3914. https://doi.org/10.1016/j.biomaterials.2009.04.009.

Singla, A. K., & Chawla, M. (2001). Chitosan: Some pharmaceutical and biological aspects-an update. *Journal of Controlled Release.* 90(3), 261-280.

Skaugrud, O. (1991) Chitosan – New biopolymer for cosmetics and drugs. *Drug Cosmetic Ind*. 148: 24–29.

Smith, E. A., Gorkum, M.C. & Dea, P.K. (2010). Properties of phosphatidylcholine in the presence of its monofluorinated analogue. *Biophysical Chemistry*. 147 (1-2), 20-27. https://doi.org/10.1016/j.bpc.2009.12.005.

Sonvico, F., Dubernet, C., Colombo, P. & Couvreur, P. (2005) Metallic Colloid Nanotechnology, Applications in Diagnosis and Therapeutics. Current Pharmaceutical Design, 11, 2095-2105.

Tadavarthy, S. M., Moller, J. H. & Amplatz, K. (1975). Polyvinyl alcohol (Ivalon)--a new embolic material. *Am J Roentgenol Radium Ther Nucl Med.* 125(3):609-16.

Tadros, T. (2010). Rheology of dispersions: principles and applications.

Tadros, T. (2014). Chapter 2 - Colloid and interface aspects of pharmaceutical science. In H. Ohshima & K. Makino (Eds.), *Colloid and Interface Science in Pharmaceutical Research and Development* (pp. 29-54). Amsterdam: Elsevier.

Tan, H., Chu, C. R., Payne, K., & Marra, K. G. (2009). Injectable in situ forming biodegradable chitosan-hyaluronic acid based hydrogels for cartilage tissue engineering. *Biomaterials*, *30*(13), 2499–2506. http://doi.org/10.1016/j.biomaterials.2008.12.080

Thanh, N.T. (2011). *Magnetic Nanoparticles: From Fabrication to Medical and Clinical Applications*. CRC Press.

Trefalt H., & Borkovec M. (2014). Overview of DLVO theory, www.colloid.ch/dlvo.

Torchilin, V. P. (2005), Recent advances with liposomes as pharmaceutical carriers. *Nature reviews drug discovery,* 4, 145-160.

Tubbs, R. K. (1966), Sequence distribution of partially hydrolyzed poly(vinyl acetate). *J. Polym. Sci. A-1 Polym. Chem.,* 4: 623-629. doi:10.1002/pol.1966.150040316

Verwey, E. J. W. (1947). Theory of the stability of lyophobic colloids. *The Journal of Physical and Colloid Chemistry. 51* (3), 631-636. DOI: 10.1021/j150453a001

Watson, H. (2015). Biological membranes. *Essays in Biochemistry*, *59*, 43–69. http://doi.org/10.1042/bse0590043

Weerd, J. Van, Karperien, M., & Jonkheijm, P. (2015). Supported Lipid Bilayers for the Generation of Dynamic Cell – Material Interfaces, 2743–2779. http://doi.org/10.1002/adhm.201500398

Wilson, D. I., (2018). What is rheology? *Eye* 32,179–183. https://doi.org/10.1038/eye.2017.267.

Younes, I. & Rinaudo, M. (2015). Chitin and chitosan: Preparation from marine sources. structure, properties and applications. *Marine Drugs*, *13*(3), 1133–1174. http://doi.org/10.3390/md13031133

Yousefi, N., & Tufenkji, N. (2016). Probing the Interaction between Nanoparticles and Lipid Membranes by Quartz Crystal Microbalance with Dissipation Monitoring. *Frontiers in Chemistry*, *4*, 46. http://doi.org/10.3389/fchem.2016.00046

Zeta-Meter Applications Brochures; Zeta-Meter, Inc.: Staunton, VA, 1

Url-1: <*http://www.androspharma.com/en/technology_en.htm*>, date retrieved 24.06.2018.

Url-2: <*http://pslc.ws/macrog/pva.htm*>, date retrieved 24.06.2018.

Url-3: <*http://pslc.ws/macrog/pva.htm*>, date retrieved 24.06.2018.

Url-4: <*https://avantilipids.com/product/840054* >, date retrieved 28.06.2018.

Url-5: <*https://avantilipids.com/product/840032*>, date retrieved 28.06.2018.

Url-6: <*https://avantilipids.com/product/890890*>, date retrieved 28.06.2018.

APPENDICES

APPENDIX A: 0.01 M, pH 7.4 Phosphate buffer saline preparing

APPENDIX A

Phosphate Buffer Saline 0.01 M pH 7.4 (PBS)

8 g NaCI

0.2 g KCI

1.44 g Na_2HPO_4

0.24 g KH_2PO_4

are dissolved 1000mL water. pH is adjusted 7.4 with NaOH or HCI.

CURRICULUM VITAE

PHOTO

Name Surname **: Arife KUŞBAZ**

Place and Date of Birth **: Sivas/ 12.06.1994**

E-Mail **: arifekusbaz@gmail.com**

EDUCATION **:**

- **B.Sc.** **:** Istanbul Technical University, Science & Letters Faculty, Department of Chemistry

PROFESSIONAL EXPERIENCE AND REWARDS:

- 5th International Bahcesehir University Drug Design Congress, "Colloidal properties and interactions of chitosan coated SPIONs with liposome layer by QCM-D technique for targeted drug delivery", 3th Best Poster Presentation award.

PUBLICATIONS, PRESENTATIONS AND PATENTS ON THE THESIS:.

5th International Bahcesehir University Drug Design Congress "Colloidal properties and interactions of chitosan coated SPIONs with liposome layer by QCM-D technique for targeted drug delivery", and "PVA coated SPIONs for targeted drug deliver", (*Poster Presentation)*

OTHER PUBLICATIONS, PRESENTATIONS AND PATENTS: